PERGAMON

Journal of Structural Geology 23 (2001) 1103–1121

JOURNAL OF STRUCTURAL GEOLOGY

www.elsevier.nl/locate/jstrugeo

Diachronous deformation and a strain gradient beneath the Selkirk allochthon, northern Monashee complex, southeastern Canadian Cordillera

James L. Crowley[a,*], Richard L. Brown[a], Randall R. Parrish[b]

[a]*Department of Earth Sciences and Ottawa–Carleton Geoscience Centre, Carleton University, Ottawa, Ontario, Canada K1S 5B6*
[b]*NERC Isotope Geosciences Centre, Keyworth NG21 5GG, UK*

Received 12 January 1999; accepted 14 September 2000

Abstract

Structural relationships of granitoid rocks dated by the U–Pb method indicate that deformation was diachronous and a strain gradient exists in a 6-km-thick section beneath the Selkirk allochthon, in the northern Monashee complex, one of the deepest structural exposures in the southern Canadian Cordillera. At high structural levels, immediately beneath a crustal-scale thrust zone that transported the allochthon eastward, a metasedimentary-dominated cover sequence was strongly affected by kilometre-scale east-verging isoclinal folds (F_1) and outcrop-scale folds (F_2) that are associated with the dominant foliation and lineation. The F_2 folding occurred, at least in part, after 58 Ma and ceased by 55 Ma. In deeper levels of the cover sequence and the underlying orthogneiss-dominated basement, F_2 folding occurred, at least in part, after 52 Ma and ceased by 49 Ma. Proterozoic dykes in the basement were locally weakly affected by D_2. These new findings require that: (i) D_2 compression youngs structurally downward, synchronous with the thermal peak of metamorphism; (ii) D_2 in deeper levels is synchronous with extension above the complex that was partly responsible for its exhumation; and (iii) a D_2 strain gradient lies between strongly deformed cover rocks and weakly D_2-deformed basement rocks. We propose a model in which rocks that were tectonised at different places and times within the orogen were juxtaposed, likely during east-verging kilometre-scale F_1 folding and shearing along the isocline limbs (a similar model was previously proposed to explain a pattern of downward younging thermal peak ages and an inverted metamorphic sequence in higher rocks). The rapid downward decrease in deformation intensity suggests that the lower limit of significant Cordilleran strain lies in the exposed basement. Cessation of deformation at this level is attributed to the fact that the basement attained elevated temperatures and began straining when the Cordilleran tectonic regime changed from compressional to extensional.

1. Introduction

The Monashee complex contains Paleoproterozoic basement rocks and overlying cover rocks in the metamorphic core of the southern Canadian Cordillera (Figs. 1 and 2). It is a tectonic window through the Selkirk allochthon, which is separated from the complex by a crustal-scale ductile thrust fault, Monashee décollement (Brown, 1980; Read and Brown, 1981; Journeay, 1986; Scammell, 1986; McNicoll and Brown, 1995), which is correlated with the sole thrust of the Rocky Mountain Foreland Belt (Brown et al., 1992; Cook et al., 1992). Cordilleran orogenesis in the northern part of the complex resulted in middle and upper amphibolite facies metamorphism, kilometre-scale isoclinal folds, and penetrative planar and linear deformation fabrics (Journeay, 1986 and references therein). The age and nature of such features at this structural level, perhaps the deepest exposed in the southern Canadian Cordillera, have significant bearing on tectonic models for the metamorphic core of the orogen.

Recent work in a 6-km-thick section in the northern Monashee complex has documented a pattern of progressive younging of thermal peak metamorphic ages with increasing structural depth (Parrish, 1995; Crowley and Parrish, 1999; Gibson et al., 1999). Gibson et al. (1999) attributed the age pattern and an inverted metamorphic field gradient in the uppermost part of the section (Journeay, 1986) to synmetamorphic non-coaxial deformation in which presently higher structural levels were transported eastward relative to deeper levels. Important aspects of this model,

* Corresponding author. Now at: Department of Earth Sciences, Memorial University of Newfoundland, St. John's, Newfoundland, Canada A1B 3X5. Tel.: +1-709-737-3046; fax: +1-709-737-2589.
E-mail address: jcrowley@sparky2.esc.mun.ca (J.L. Crowley).

0191-8141/01/$ - see front matter
PII: S0191-8141(00)00179-6

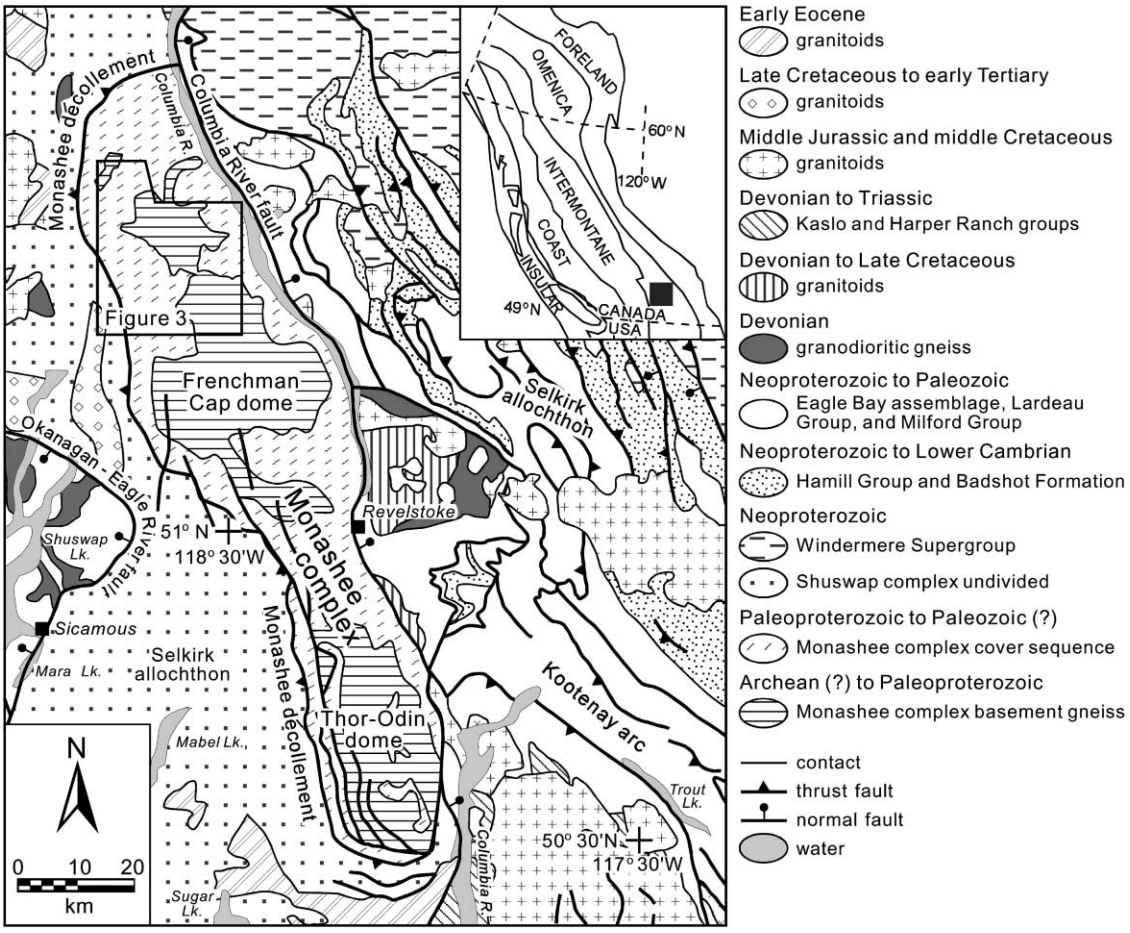

Fig. 1. Tectonic assemblage map in the vicinity of the Monashee complex, modified after Wheeler and McFeely (1991), showing the location of Fig. 3. The dark grey square in inset locates the map with respect to the morphogeologic belts of the Canadian Cordillera.

which have not been previously documented, are that: (i) deformation was synchronous with the downward younging thermal peak, and (ii) a strain gradient exists in the section, beneath which the rocks have been weakly deformed during Cordilleran orogenesis.

We present new U–Pb ages from granitoid rocks with key structural relationships and synthesize our previously published ages in order to show that evidence exists in the northern Monashee complex for diachronous deformation, which was synchronous with the thermal peak, and a strain gradient. A rapid downward decrease in deformation intensity supports the contention that the complex is autochthonous, and thus has always been part of the North American craton (Crowley, 1999 and references therein). Based on our new findings, we propose a tectonic model that is modified after Gibson et al. (1999), taking into consideration the timing and intensity of deformation and data from deeper structural levels. For example, we show that compressional deformation at deep levels of the complex was synchronous with extension above the complex that was partly responsible for its exhumation.

2. Geological setting

The Monashee complex lies in the southern Omineca Belt, the metamorphic and plutonic hinterland to the Rocky Mountain Foreland Belt of the Canadian Cordillera that developed subsequent to collision between accreted terranes and the western edge of the North American craton (Monger et al., 1982). The complex contains one of three Paleoproterozoic (~2.2–1.8 Ga) crystalline basement exposures in the Canadian Cordillera (Crowley, 1999 and references therein). Basement para- and ortho-gneisses form the core of two structural culminations in the complex (Fig. 1), the Frenchman Cap dome to the north and the Thor–Odin dome to the south. The basement is unconformably overlain by the cover sequence, a platformal succession of metasedimentary and subordinate metaigneous rocks that is 2–3 km thick and laterally extensive (Scammell and Brown, 1990 and references therein). The cover sequence has been dated as Paleoproterozoic at the base, pre-Neoproterozoic in the lower part (Crowley, 1997), and Cambrian in the middle (Höy and Godwin, 1988).

The Monashee décollement, a ductile fault zone up to

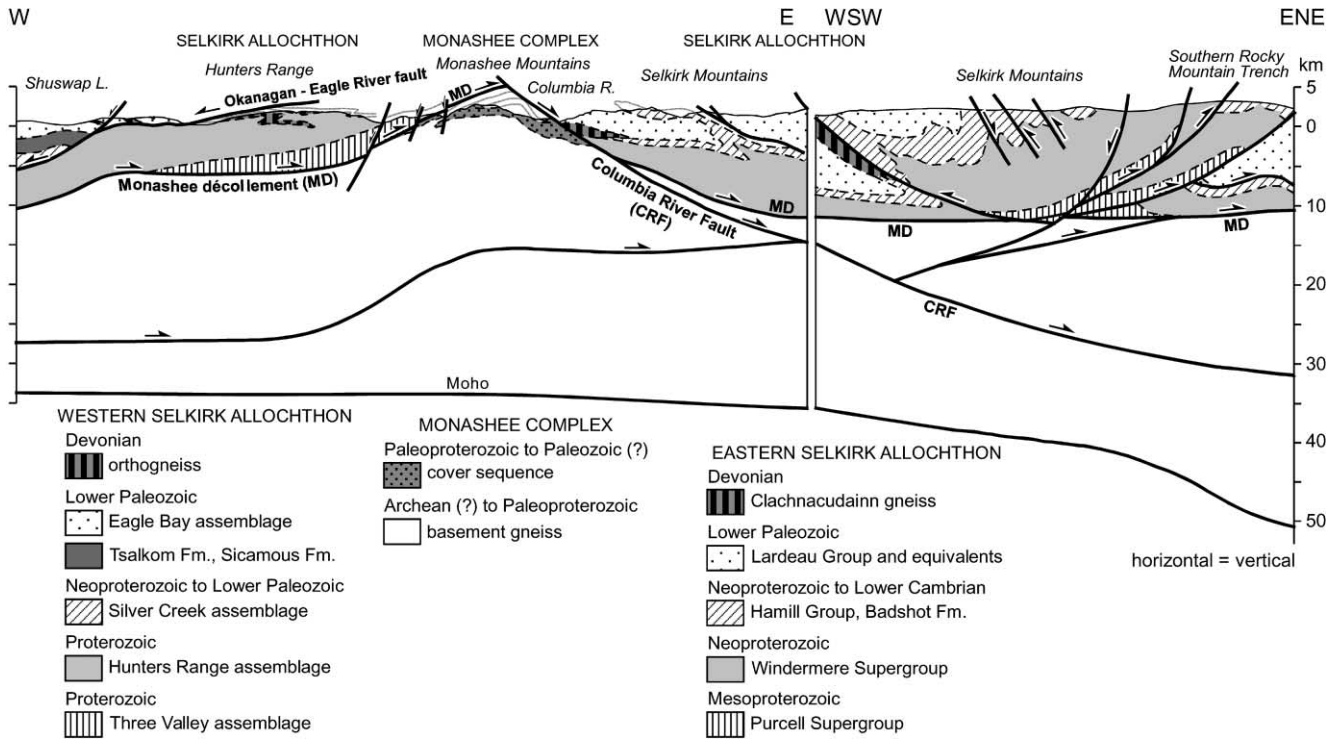

Fig. 2. Crustal cross-section through the southern Omineca Belt, taken from Johnson and Brown (1996). The section transects the Monashee complex through the northern part of the Thor–Odin dome (for exact location see fig. 2 in Johnson and Brown).

1 km thick, was mapped between the Monashee complex and the overlying Selkirk allochthon (Brown, 1980; Read and Brown, 1981; Journeay, 1986; Scammell, 1986; McNicoll and Brown, 1995) (Figs. 1–3) This structure was interpreted as regionally significant, largely on the basis that kilometre-scale folds in the complex are truncated at the décollement and it juxtaposes different lithologies. Kinematic indicators suggest top-to-the-east motion on the décollement's west dipping surface, leading to its interpretation as a thrust fault. Higher grade mineral assemblages and greater proportion of leucogranitic rocks in the allochthon suggested that it originated at deeper levels than the structurally underlying complex. U–Pb dating of leucogranitic rocks showed that the décollement on the south flank of the Thor–Odin dome was active shortly before 58 Ma (Carr, 1992). Surface geology and Lithoprobe seismic reflection profiles were used to correlate the décollement with the Late Cretaceous–Paleocene basal thrust beneath the Rocky Mountain Foreland Belt, and thus it was considered to be a structure that links middle crustal strain in the hinterland of the orogen with upper crustal strain in the foreland (Brown et al., 1992; Cook et al., 1992 and references therein). Palinspastic restoration of the Selkirk allochthon indicates up to ~300 km of northeastward displacement relative to the North American craton (Brown et al., 1993), with >80 km of that occurring on the décollement (Read and Brown, 1981; Brown et al., 1986).

The Selkirk allochthon has a protracted, multiple-event history spanning more than 100 My, from Early Jurassic in the highest structural level to early Tertiary in the lowest (Parrish, 1995 and references therein). Parrish considered this history to be consistent with the thermal evolution of rocks in the hinterland of a fold and thrust belt that were progressively buried under the belt as it propagated toward the foreland. The allochthon's protracted history contrasts with the relatively simple Cordilleran history of the Monashee complex, where only one thermal event (early Tertiary) is recorded and Mesozoic igneous rocks have not been found. These characteristics were used to contend that the complex was part of the craton and overlying foreland basin in the Mesozoic, while the allochthon was being deformed and metamorphosed to the west of its present position. In addition, the complex did not attain peak thermal conditions until the allochthon's hot base was thrust eastward onto it during Late Cretaceous–early Tertiary motion on the décollement. In this model, warmer rocks progressively overrode cooler rocks as displacement migrated forward, synchronous with cooling and exhumation of previously tectonized rocks at higher levels.

Compressional tectonism in the southern Omineca Belt was followed shortly thereafter by extension of the orogen (Parrish et al., 1988 and references therein). The east margin of the complex is defined by the Columbia River fault (Figs. 1 and 2), an Eocene brittle–ductile normal fault that is superposed on the Monashee décollement (Lane, 1984 and references therein). The Columbia River fault displacement has been estimated at <10 km (Lane, 1984) and >15 km (Parrish et al., 1988; Johnson and Brown, 1996). This fault and a

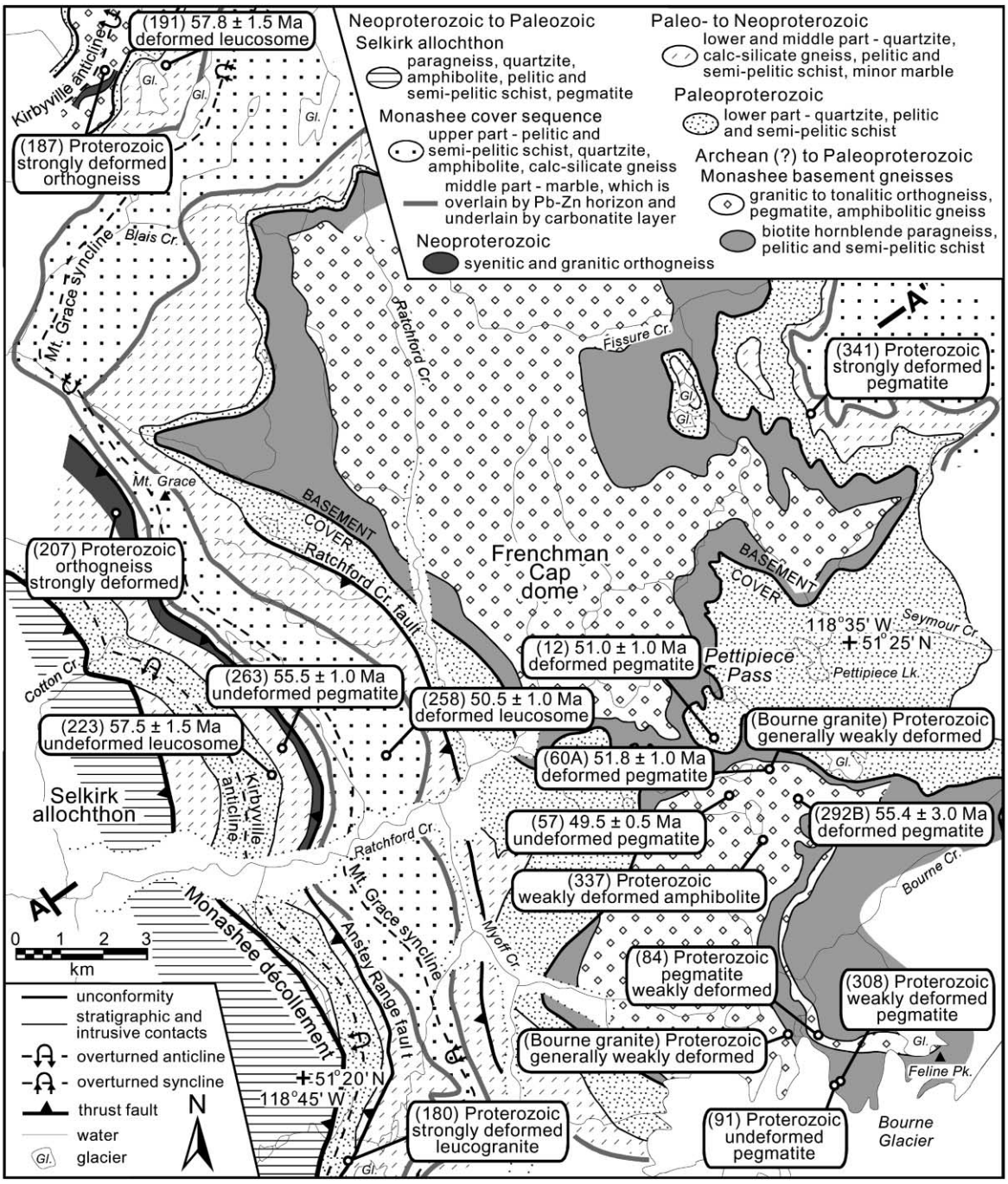

Fig. 3. Geologic map of the northern part of Frenchman Cap dome, modified after Wheeler (1965), Höy and Brown (1980) and Journeay (1986) showing localities of samples with U–Pb ages (sample numbers are shown in parentheses). Descriptions of intensity of deformation are made with respect to synmetamorphic Cordilleran (D_2) deformation. Line A–A′ locates the cross-section in Fig. 4.

coeval normal fault to the west, the Okanagan–Eagle River system (Figs. 1 and 2), bound the Shuswap metamorphic complex. Displacement on them resulted in rapid exhumation of the Monashee complex and arching of the décollement (Brown and Journeay, 1987; Parrish et al., 1988).

2.1. Metamorphism

The Frenchman Cap basement was metamorphosed at ~2.06 Ga (Crowley, 1999), before deposition of an unconformably overlying cover sequence. Basement and cover were metamorphosed during Cordilleran orogenesis. Metamorphic mineral assemblages in pelitic schist in the north-central part (Pettipiece Pass area) of the dome (Journeay, 1986 and references therein) indicate that: (i) the highest grade rocks (sillimanite–K-feldspar assemblage) exist at the structurally highest level, (ii) the lowest grade rocks (sillimanite–kyanite–staurolite–muscovite

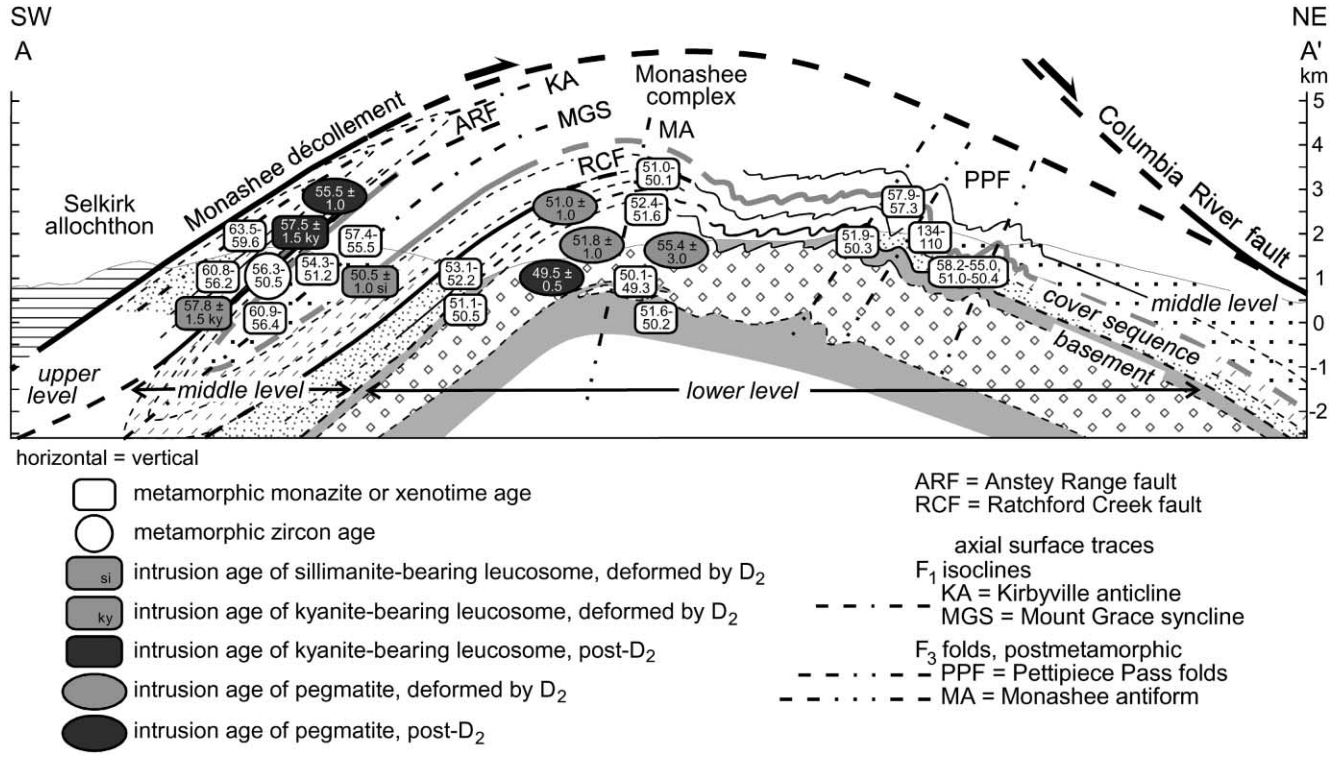

Fig. 4. Cross-section of the northern part of the Frenchman Cap dome, modified after Journeay (1986), showing approximate structural position of samples with U–Pb ages (in Ma). Location of section and patterns for rock units are shown in Fig. 3. D_2, synmetamorphic Cordilleran deformation

assemblage) exist at an intermediate structural level, and (iii) the lowest grade rocks are underlain by higher grade rocks (sillimanite–kyanite–muscovite assemblage) (see fig. 3 in Crowley and Parrish (1999)).

Journeay (1986) used petrographic data to contend that metamorphism in the dome occurred during two distinct events: (i) an intermediate pressure event, during which kyanite, staurolite, and sillimanite grew; and (ii) a low pressure overprint, during which andalusite and sillimanite replaced kyanite and sillimanite–K-feldspar assemblages grew in the highest temperature schists. The older event affected the entire dome and was associated with a normal thermal gradient (i.e. warmer rocks overlain by cooler rocks), whereas the overprint affected only the structurally highest rocks and was associated with an inverted gradient (i.e. cooler rocks were overlain by warmer rocks). The heat source for the inverted gradient was interpreted as the base of the Selkirk allochthon as it was thrust onto the dome.

U–Pb dates of 78–49 Ma from various minerals and rock types in high structural levels of the Frenchman Cap and Thor–Odin domes were interpreted as indicating elevated temperatures during this period (Coleman, 1990; Parkinson, 1992; Carr, 1995; Parrish, 1995; Gibson, 1997; Crowley and Parrish, 1999). The lack of isotopic data indicating Phanerozoic magmatism, metamorphism, or migmatization in basement rocks in the Frenchman Cap dome allowed Armstrong et al. (1991) to conclude that these rocks were weakly affected by Cordilleran metamorphism. Sanborn (1996) used hornblende and biotite $^{40}Ar/^{39}Ar$ dates from the dome to show that the cover sequence cooled rapidly in the early Tertiary. Based on U–Pb dates from throughout the southern Omineca belt, Parrish (1995) constructed a model in which the complex was at low temperatures in the Mesozoic and located east (on the foreland side) of the metamorphic front. Elevated temperatures were not attained until the warmer Selkirk allochthon was emplaced onto it in the Late Cretaceous–early Tertiary. The metamorphism was attributed to a single event that was associated with an inverted thermal gradient, with the heat having been transferred down from the Selkirk allochthon as it was thrust onto the complex. This conclusion was based on the short duration of the event (<5 My based on modeling Pb diffusion from Proterozoic titanite) and the fact that the base of the allochthon was at higher temperatures than the complex during the event (based on mineral assemblages (Brown, 1980; Journeay, 1986; Scammell, 1986) and U–Pb dating (Parrish, 1995 and references therein)).

Crowley and Parrish (1999) used U–Pb data to contend that the Cordilleran thermal peak in the Pettipiece Pass area of Frenchman Cap dome youngs structurally downward and the rocks were significantly heated only once in the Phanerozoic. Xenotime and monazite dates vary progressively from 64 Ma in the highest level to 49 Ma in the deepest level. These dates were interpreted as closely reflecting growth ages rather than cooling ages or

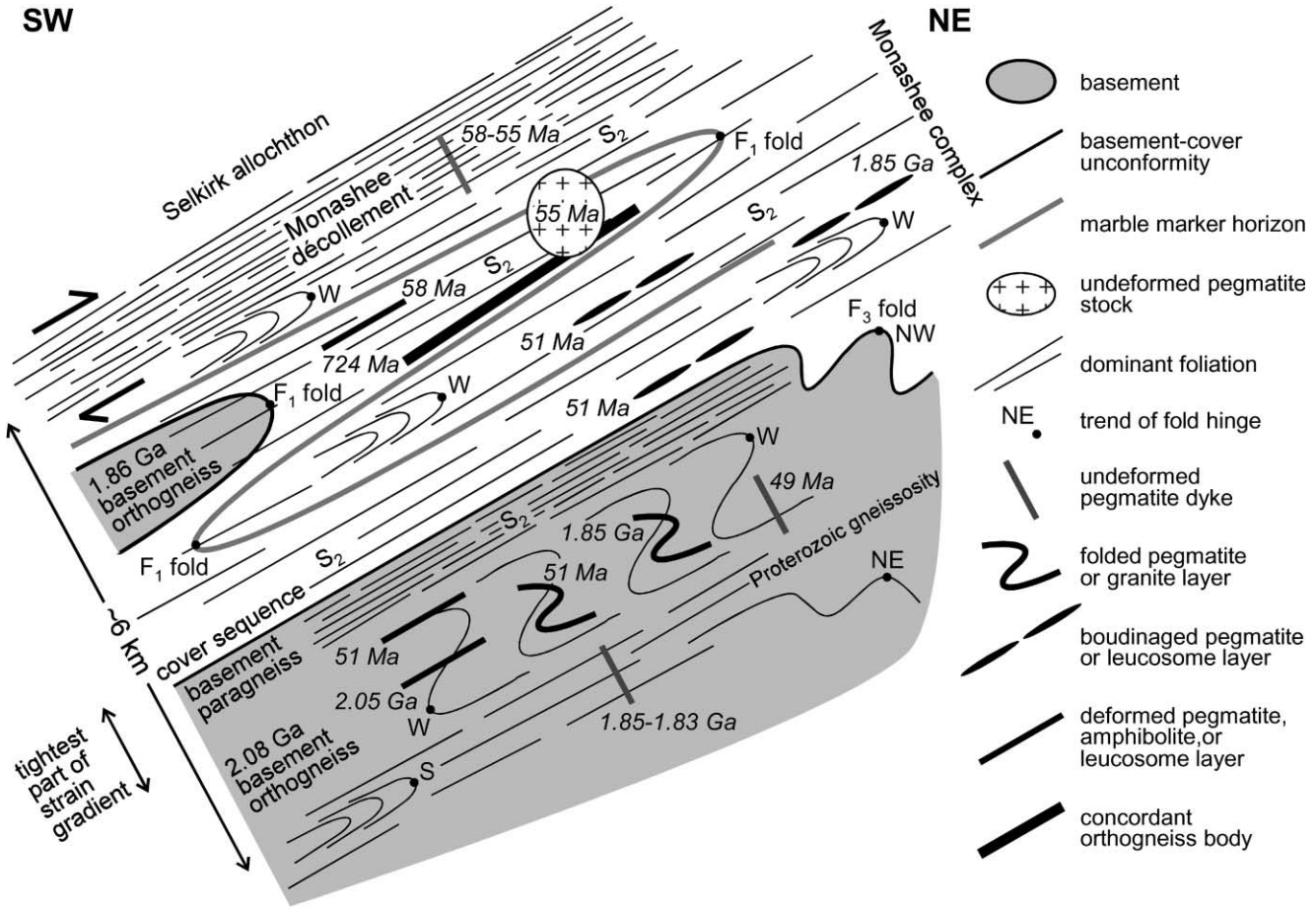

Fig. 5. Schematic cross-section depicting the structural relationships of the dated granitoid rocks.

substantially reset ages based on the lack of Pb diffusion in Proterozoic monazite. This inference was supported by $^{40}Ar/^{39}Ar$ data (Sanborn, 1996) that suggested rapid cooling occurred immediately after growth. The negligible-to-moderate amounts of diffusive Pb loss in Proterozoic monazite and titanite in deeper rocks were considered in the light of previous studies of Pb diffusion to contend that elevated temperatures (~600–650°C are inferred from pelitic mineral assemblages) existed in these rocks for a short duration, perhaps only a few million years. The growth ages were interpreted as thermal peak ages based on U–Pb dates from coeval kyanite-bearing leucosomes, the consistent nature of the U–Pb dates throughout the study area, and petrographic relationships that suggest monazite grew before or during development of S_2. These findings led to the conclusion that metamorphism was diachronous according to structural level, with higher rocks attaining peak temperatures and cooling rapidly while deeper rocks were heating toward a thermal peak that was attained a few million years later. This scenario requires that structurally higher rocks cannot have been the heat source for the deeper metamorphism, as previously proposed (Journeay, 1986; Parrish, 1995).

2.2. Deformation

The following summary of deformation in the Frenchman Cap dome is based on work by Wheeler (1965), Höy and Brown (1980), Journeay (1986), Scammell (1986), Crowley (1999) and this study. Although the following terminology (F_1, F_2, etc.) is based on the history of the cover sequence, folds and fabrics in the basement that are interpreted as being cogenerational with those in the cover, based on style and orientation of the structural elements, are given the same name.

The dominant gneissosity in some basement exposures formed before 1.85 Ga, prior to deposition of the cover sequence. The largest and oldest recognized Cordilleran structures are east-verging kilometre-scale recumbent isoclines, termed F_1 isoclines, on the west side of the dome. The two deepest F_1 isoclines, the Mount Grace syncline and Kirbyville anticline (Figs. 3 and 4)., are exposed in the study area. They are overlain to the north by the Sibley Creek syncline and an overlying anticline. The Kirbyville anticline is cored by the westernmost exposure of basement in the dome. In contrast, basement in the centre of the dome does not core F_1 isoclines; the unconformity is a

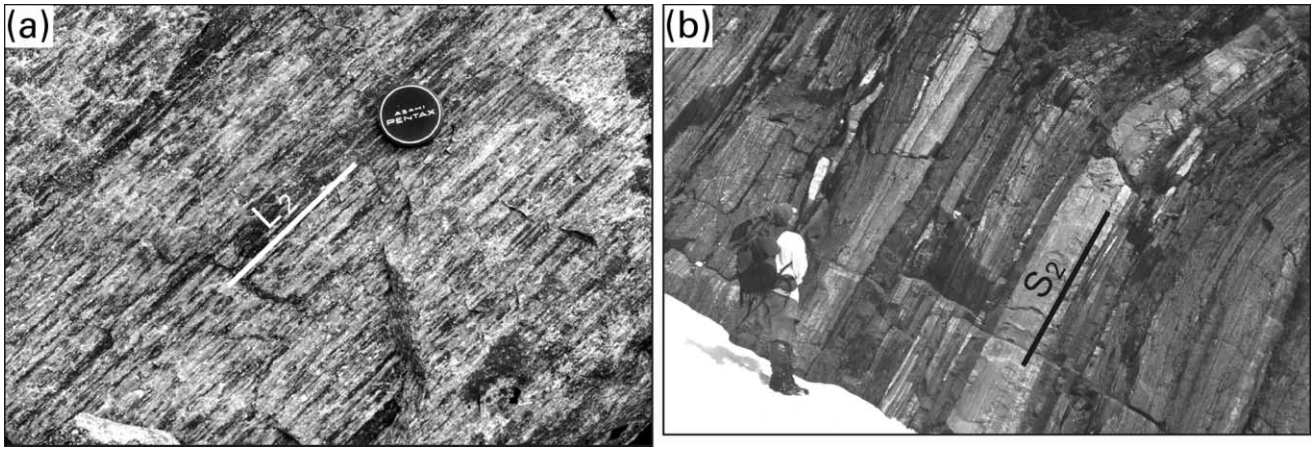

Fig. 6. D_2 fabrics in Proterozoic rocks. (a) View perpendicular to S_2 in sample 207, a Neoproterozoic orthogneiss (upper structural level), showing a strong L_2. (b) S_2 in basement paragneiss that lies immediately beneath the cover sequence (upper part of lower structural level). View is to the northeast. A drastically different structural setting exists in basement orthogneiss beneath this section, where a Proterozoic gneissosity is well-preserved and D_2 had locally minor effects (see Figs. 12 and 13; Crowley, 1999).

simple domed surface that is locally warped by minor post-metamorphic folds (F_3 folds, see below). The lack of F_1 folding of this part of the unconformity may indicate that it lies along the limb of an F_1 isocline or that there was minor F_1-related strain in this structural level. The observations that F_1 isoclines do not fold the isograds and are truncated at the Monashee décollement led to the conclusion that the isoclines began forming before peak metamorphism and synmetamorphic motion on the décollement. Sheared surfaces along the limbs of the Mount Grace and Kirbyville folds are the Ratchford Creek and Anstey Range faults, respectively (Figs. 3 and 4).

Synmetamorphic F_2 folds are the most prevalent outcrop-scale structures in the dome and are associated with the dominant Cordilleran fabrics. The S_2 foliation (gneissosity in metaigneous rocks and schistosity in pelitic and semi-pelitic schists) is axial planar to F_2 folds and conforms to the domal shape of the Frenchman Cap culmination. Elongate minerals in pelitic schists (e.g. sillimanite and kyanite), stretched mineral aggregates (e.g. quartz and feldspar), stretched quartzite pebbles in conglomerates, and the intersection between S_2 and compositional layering are coaxial with the hinge lines of F_2 folds. These linear elements, collectively termed L_2, generally have a down-dip orientation within S_2 (i.e. they plunge to the west-southwest on the west side of the dome and to the east-northeast on the east side of the dome). Amphibolite layers are locally boudinaged in a direction parallel to L_2. F_2 folds are associated with map-scale fold closures in only one locality (the southwest part of the study area). Because the F_2 folds are rootless intrafolial structures, an overall sense of vergence has not been determined. The sense of shear during formation of the D_2 fabrics has also not been determined, with the exception of east-northeasterly-directed fabrics adjacent to the Monashee décollement. Given that F_2 folds have: (i) an apparently ambiguous sense of vergence, (ii) shallow-dipping axial surfaces, and (iii) axes that lie parallel to the dominant stretching direction, it is likely that D_2 was a phase of significant vertical flattening and east–west stretching. Postmetamorphic F_3 folds are

Fig. 7. Sample 258 (~51 Ma, Crowley and Parrish (1999)) is from a leucosome layer (denoted by arrow) that is boudinaged and concordant with S_2 in the host amphibolitic gneiss. This layer and similar layers in the outcrop intruded into the middle structural level. These relationships suggest that D_2 occurred, at least in part, after leucosome crystallization at ~51 Ma. View is to the north. At a higher structural level, S_2 had ceased forming before ~56 Ma (see Fig. 9).

Table 1
U–Pb analytical data

Analysis[a]		Weight[b] (μg)	U (ppm)	Pb*[c] (ppm)	$^{206}Pb/^{204}Pb$[d]	Pb_c[e] (pg)	^{208}Pb[f] (%)	$^{206}Pb/^{238}U$[g]	$^{207}Pb/^{235}U$[g]	Correlation coefficient	$^{207}Pb/^{206}Pb$[g]	$^{207}Pb/^{206}Pb$ age[h] (Ma)
Sample 12 (Fig. 8b). Adjacent pegmatite and aplite layers, 0.5 km thick, boudinaged, concordant or nearly so with S_2, intruded into lower part of cover sequence; located 1.4 km south of Pettipiece Pass at 2200 m, 387480E-5695060N												
A*	4,105,L1	15	9915	70.2	2249	34	0.2	0.007853 ± 0.13	0.05139 ± 0.16	0.88	0.04746 ± 0.08	72.4 ± 3.6
B*	9,74,t,L1	10	8967	63.67	2787	16	0.2	0.007875 ± 0.10	0.05154 ± 0.14	0.79	0.04747 ± 0.09	73.1 ± 4.2
C	3,105,L1	23	17833	126	2105	97	0.3	0.007828 ± 0.19	0.05121 ± 0.20	0.80	0.04744 ± 0.12	71.6 ± 5.9
D	3,105,L2	18	9260	66.66	1777	47	0.3	0.007978 ± 0.16	0.05189 ± 0.27	0.54	0.04718 ± 0.23	58.2 ± 10.9
E	3,105,L2	16	6768	48.78	2165	26	0.2	0.007989 ± 0.10	0.05216 ± 0.14	0.79	0.04735 ± 0.09	67.0 ± 4.2
F	3,105,L2	22	8128	58.26	3374	27	0.2	0.007952 ± 0.10	0.05188 ± 0.12	0.88	0.04732 ± 0.06	65.2 ± 2.7
Sample 57 (Fig. 8b). Pegmatite dyke, 0.7 m thick, undeformed, intruded into basement orthogneiss; located 2.8 km south of Pettipiece Pass at 2080 m, 387830E-5693680N												
A*	1,105,t,cs	14	20630	145.6	7585	18	0.5	0.007805 ± 0.15	0.05097 ± 0.16	0.97	0.04736 ± 0.04	67.4 ± 1.9
B*	6,74,cs	3	11957	84.69	1826	11	0.4	0.007836 ± 0.12	0.05140 ± 0.22	0.61	0.04757 ± 0.17	78.1 ± 8.3
C	1,149,tn	27	16614	116.7	1583	140	0.5	0.007763 ± 0.28	0.05092 ± 0.30	0.73	0.04757 ± 0.21	78.1 ± 10.1
D	2,105,tn	10	12333	87.57	599	101	0.2	0.007868 ± 0.18	0.05199 ± 0.74	0.40	0.04792 ± 0.68	95.3 ± 32.4
E	6,74,cs	6	10862	75.43	270	134	0.1	0.007709 ± 0.29	0.04986 ± 0.88	0.63	0.04691 ± 0.74	44.7 ± 35.3
F	3,74,t,tn	4	21408	150.1	1158	40	0.3	0.007765 ± 0.11	0.05061 ± 0.19	0.71	0.04727 ± 0.14	62.9 ± 6.5
G	9,74,cs	17	2079	14.67	1010	18	0.4	0.007807 ± 0.10	0.05124 ± 0.22	0.61	0.04760 ± 0.18	79.5 ± 8.4
Sample 60A (Fig. 8c). Pegmatite layer, 0.5 m thick, F_2 folded and contains S_2, intruded into basement orthogneiss; located 2.7 km south-southeast of Pettipiece Pass at 2130 m, 387480E-5695064N												
A*	3,149	39	7419	57.01	12372	13	0.1	0.008501 ± 0.13	0.05993 ± 0.14	0.97	0.05113 ± 0.04	246.7 ± 1.6
B*	3,105	26	3842	35.56	5230	12	0.3	0.010127 ± 0.11	0.08372 ± 0.12	0.91	0.05996 ± 0.05	602.1 ± 2.3
C*	5,105,t	24	5097	40.19	2832	24	0.2	0.008697 ± 0.10	0.06383 ± 0.13	0.88	0.05323 ± 0.06	338.8 ± 2.7
D	4,105,t	14	5767	44.63	1070	42	0.1	0.008565 ± 0.12	0.06006 ± 0.31	0.47	0.05086 ± 0.28	234.3 ± 12.8
E	6,74	12	5733	46.75	2149	19	0.1	0.008991 ± 0.11	0.06708 ± 0.15	0.81	0.05411 ± 0.09	375.6 ± 4.1
F	6,74,t	22	10034	74.22	4937	24	0.0	0.008210 ± 0.17	0.05475 ± 0.18	0.96	0.04836 ± 0.05	117.0 ± 2.2
Sample 263 (Fig. 8a). Pegmatite stock, 0.5 km diameter, undeformed, intruded into lower part of cover sequence; located 7.5 km southeast of Mount Grace at 1290 m, 376750E-5693840N												
A	3,149	52	2437	19.36	9139	8	1.6	0.008686 ± 0.15	0.05654 ± 0.15	0.78	0.04721 ± 0.10	59.6 ± 4.8
B	3,149	39	1514	12.9	1989	16	10.1	0.008501 ± 0.11	0.05541 ± 0.17	0.68	0.04727 ± 0.12	63.0 ± 5.9
C	3,149	50	1439	11.52	3023	13	1.1	0.008817 ± 0.11	0.05758 ± 0.17	0.62	0.04737 ± 0.14	67.7 ± 6.5
D	7,105	48	1445	11.6	4352	9	2.1	0.008730 ± 0.10	0.05681 ± 0.14	0.73	0.04719 ± 0.10	59.1 ± 5.4
Sample 292B (Fig. 8d). Pegmatite layer, 0.3 m thick, F_2 folded and contains S_2, intruded into basement orthogneiss; located 3.7 km southeast of Pettipiece Pass at 2300 m, 389350E-5693440N												
A	2,105,cs,t	24	1413	105.9	3425	46	1.0	0.078096 ± 0.29	1.13568 ± 0.30	0.99	0.10547 ± 0.04	1722.5 ± 1.6
B	4,74,cs,t	15	1968	144.3	11657	12	0.9	0.076595 ± 0.18	1.09484 ± 0.19	0.99	0.10367 ± 0.03	1690.8 ± 1.2
C	1,149,tn,t	13	5805	97.39	1752	50	1.3	0.017835 ± 0.11	0.19845 ± 0.14	0.90	0.08070 ± 0.06	1214.1 ± 2.3
D	1,105,tn	6	1578	242.8	4106	23	2.3	0.157603 ± 0.12	2.38890 ± 0.13	0.96	0.10993 ± 0.04	1798.3 ± 1.4
E	5,74,cs,t	17	1450	30.1	1877	18	0.9	0.022061 ± 0.10	0.26026 ± 0.15	0.75	0.08556 ± 0.10	1328.3 ± 3.9

Notes: isotopic composition of Carleton University laboratory blank (uncertainty is 1σ): 206:207:208:204 = 19.01 ± 0.36:15.64 ± 0.20:38.23 ± 0.74:1; UTM coordinates in grid zone 11, North American Datum 1983 (NAD83).

[a] A–G in first column, fraction codes for zircon analyses; *, chemistry done at the Geological Survey of Canada in Ottawa, Ont. (other chemistry done at Carleton University); 1–9 in second column, number of grains analyzed; 74–149, average size in μm before abrasion with pyrite (Krogh, 1982); cs, colourless; tn, tan colour; t, tips of grains; L1, layer one; L2, layer two.

[b] Weighing uncertainty is 1 μg.

[c] Radiogenic Pb.

[d] Measured ratio, corrected for spike and Pb fractionation of 0.09 ± 0.03%/a.m.u.

[e] Total common Pb in analysis, corrected for spike and fractionation.

[f] Radiogenic ^{208}Pb, expressed as percentage of total radiogenic Pb.

[g] Corrected for blank Pb and U and common Pb (Stacey–Kramers model Pb composition equivalent to the interpreted age of the analyses); errors are 1σ in percent.

[h] Errors are 2σ in Ma.

generally northeast-verging with subhorizontal hinge lines and upright to moderately inclined axial surfaces. F_3 folds are best developed in the cover sequence on the east side of the dome (Fig. 4). F_3 folds exist locally in the basement in the centre of the dome, yet are absent in the deepest levels.

At least some thrusting on the Monashee décollement on the southern flank of the Thor–Odin dome was bracketed at ~59–58 Ma based on dating of a deformed leucogranite and undeformed pegmatite (Carr, 1992). Deformation in the vicinity of the décollement on the west flank of the Frenchman Cap dome predated ~58–55 Ma pegmatite dykes (Scammell, 1993; Parrish, 1995). Deformation in 53–50 Ma pegmatites on the east flank of the Thor–Odin dome was attributed to extension on the Columbia River fault (Parkinson, 1992).

U–Pb data from the following 12 samples were reported elsewhere; three early Tertiary leucosomes were presented by Crowley and Parrish (1999) and nine Proterozoic rocks were presented by Crowley (1997, 1999) and Armstrong et al. (1991). These data are briefly summarized and shown here (Table 2, Figs. 3–5) because they have not previously been considered in discussions of Cordilleran deformation. A first set of samples comes from structurally high rocks. A 58 Ma leucosome layer (sample 191) was affected by at least some D_2, while a similar age leucosome pod (sample 223) possibly intruded after D_2. A Neoproterozoic (sample 207) (Fig. 6a) and two Paleoproterozoic granitoid rocks (samples 180 and 187) were strongly affected by D_2. A second group comes from an intermediate structural level. A 51 Ma leucosome layer (sample 258) (Fig. 7) was affected by at least some D_2 and a Paleoproterozoic pegmatite (sample 341) was strongly affected by D_2. A final set comes from the structurally deepest rocks that have drastically different structural settings. Layers and stocks of a widespread Paleoproterozoic granite (Bourne granite) were correlated on the basis of mineralogy and dates from three localities. Based on the pristine (i.e. not migmatized) appearance of the granite where it is highly discordant to the migmatitic gneissosity in the host orthogneisses, intrusion was interpreted as having postdated development of the gneissosity. The granite appears weakly deformed in outcrop because of its equigranular and homogeneous nature, but it does contain a weak to moderately developed foliation and lineation. A Paleoproterozoic amphibolite dyke (sample 337) postdates a gneissosity in the basement. Three Paleoproterozoic pegmatite dykes (samples 84, 91 and 308) that intruded into deep levels of the basement are weakly deformed to undeformed.

3. U–Pb geochronology

In the study of strongly tectonized rocks, it is difficult to determine when ductile deformation began and how the intensity of the strain varies spatially and temporally. The timing of early strain is uncertain because precise intrusion ages must be obtained from rocks that crystallized immediately before and during deformation; such structural interpretations are not straightforward and age interpretations may be difficult because of possible disruption of the U–Pb system during the subsequent thermal peak of metamorphism. These problems can potentially be solved for Cordilleran deformation in the Pettipiece Pass area of the Frenchman Cap dome for two reasons. First, the area contains the lowest grade rocks in the Monashee complex, which were shown by Crowley and Parrish (1999) to have been subjected to maximum thermal conditions that are below the Pb closure temperatures in monazite and titanite. Thus, igneous accessory minerals grown before and during the thermal peak should yield U–Pb dates that closely reflect crystallization. Second, the area contains numerous structural markers, some formed before Cordilleran deformation, such as Proterozoic granitoid rocks and ductile fabrics (Crowley, 1997, 1999), and others that developed during Cordilleran orogenesis, such as pegmatites and leucosomes (Crowley and Parrish, 1999; this paper).

We present U–Pb data from five granitoids that crystallized during Cordilleran orogenesis in the Pettipiece Pass area. Analytical data and sample locations are given in Table 1. Concordia diagrams are depicted in Fig. 8. The ages are shown on the map of Fig. 3, the cross-sections in Figs. 4 and 5, and in Table 2. For simplicity, the study area is divided into three levels according to structural distance from the Monashee décollement, which defines the west margin of the dome and is interpreted as arched over it (Journeay, 1986). The Anstey Range fault (Figs. 3 and 4) (Journeay, 1986) is the boundary between upper and middle levels, and the basement-cover unconformity separates the middle and lower levels. It is emphasized that boundaries between the levels do not have tectonic age significance because there are age overlaps across them. The structural thickness from the décollement to the deepest basement exposure is 6 km.

3.1. Analytical methods

U–Pb geochronology by the isotope dilution thermal ionization mass spectrometric method followed procedures outlined by Parrish et al. (1987): microcapsules for mineral dissolution (Parrish, 1987), a mixed ^{233}U–^{235}U–^{205}Pb tracer (Parrish and Krogh, 1987), multicollector mass spectrometry (Roddick et al., 1987), and estimation of errors using numerical error propagation (Roddick, 1987). Decay constants used are those recommended by Steiger and Jäger (1977). Discordia lines through analyses were calculated with the use of a modified York (1969) regression (Parrish et al., 1987), which takes scatter into account. The uncertainties on the upper and lower intercept ages of the discordias are the realistic errors. Mineral selection and most of the U–Pb chemistry were performed in the geochronology laboratory at Carleton University, where U blanks were less than 5 pg and Pb blanks were usually

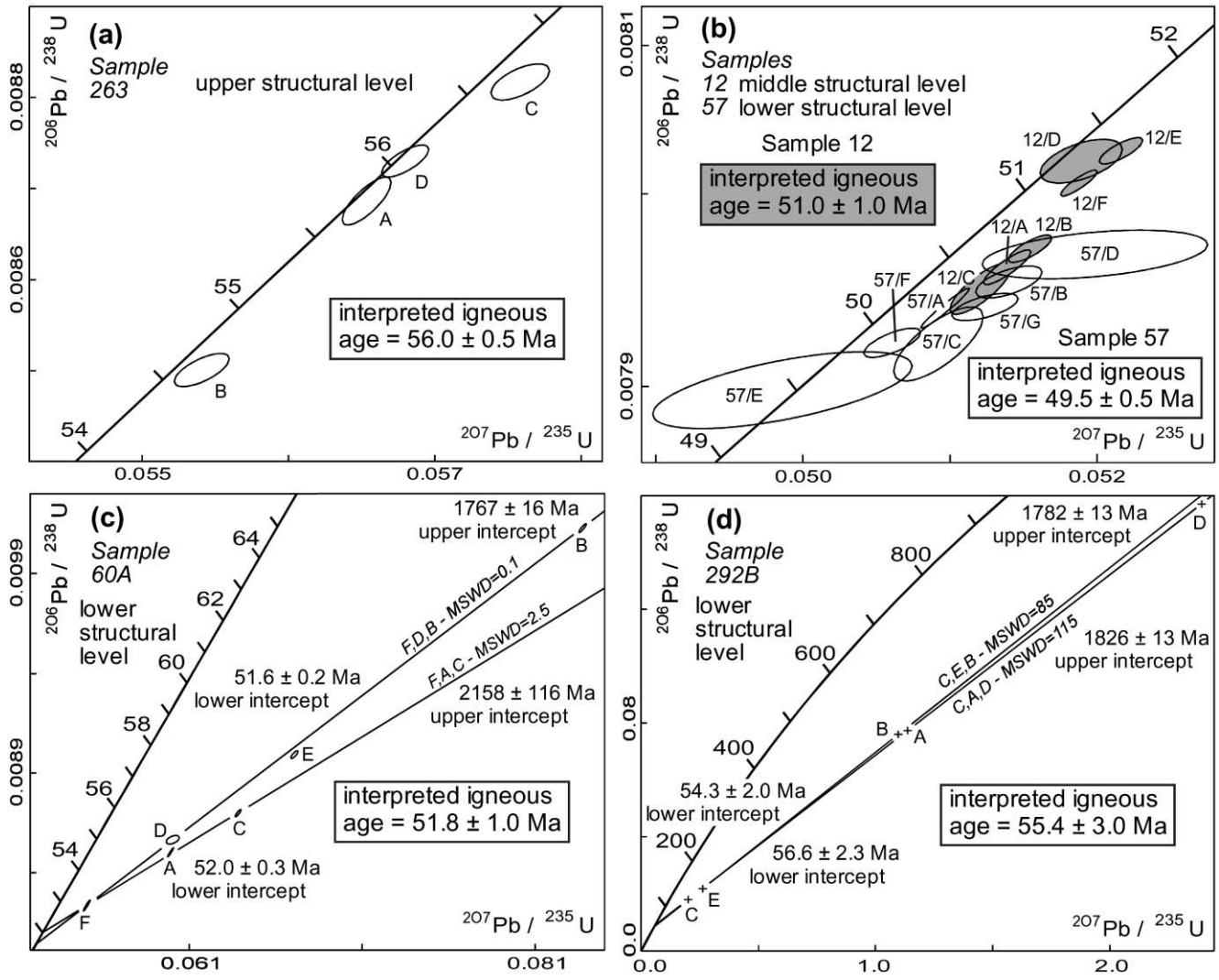

Fig. 8. U–Pb concordia plots. Ellipses for the analyses represent the two sigma uncertainty (95% confidence level) and analyses plotted with + symbols have ellipses that are too small to be seen at this scale. In (b) the analyses are identified as follows: the sample number lies to the left of the / symbol and the analysis identifier lies to the right. See Table 1 for analytical data.

5–20 pg. Other U–Pb chemistry was performed at the geochronology laboratory at the Geological Survey of Canada in Ottawa, where Pb blanks were usually 5–10 pg. Isotopic ratios were determined on a MAT 261 mass spectrometer at the Geological Survey of Canada.

The clearest and least magnetic zircons with the fewest inclusions and cracks were analysed. Grains that contain xenocrystic cores that were visible with a microscope in transmitted light were avoided. All zircons had an igneous morphology (i.e. prismatic and elongate, aspect ratios typically 3:1 to 6:1). Whole zircon grains were analysed, except for the few cases in which tips of grains that were separated from central parts of the grains were analysed. All zircons were abraded (Krogh, 1982).

3.2. Upper level

Sample 263 is from a pegmatite stock, ~0.5 km wide, which intruded into amphibolitic gneiss and schist in the lower part of the cover sequence, in the lower limb of the Kirbyville anticline south of Mount Grace (Fig. 3). The stock is devoid of deformation fabrics and its contacts are highly discordant to S_2 in the host (Fig. 9). These relationships suggest that D_2 in the host occurred before pegmatite crystallization. This stock is the largest known undeformed granitoid rock in the dome. Four analyses (three to seven grains each; Table 1) of zircons with igneous morphologies yield U–Pb dates that lie slightly below or just overlap concordia at 57.0–54.5 Ma (Fig. 8a).

3.3. Middle level

Sample 12 is from 0.5–1.0 m thick pegmatite and aplite layers that intruded into calcareous schist in the lower part of the cover sequence, south of Pettipiece Pass (Fig. 3). Most layers are concordant with S_2 in the host (including

Table 2
Summary of U–Pb ages from early Tertiary granitoid rocks

Sample	Rock type	Key relationships	Age (Ma)	Mineral[a]
Upper level				
191[b]	Leucosome	Contains Ky, Sil, and And; Ky defines L_2; concordant with S_2	57.8 ± 1.5	Zrn, Mnz
223[b]	Leucosome	Contains Ky, Sil, and And; igneous fabrics only	57.5 ± 1.5	Zrn, Mnz
263	Pegmatite	Igneous fabrics only; highly discordant to S_2	56.0 ± 0.5	Zrn
Middle level				
12	Pegmatite	Boudinaged by D_2; concordant or nearly so with S_2; F_3 folded	51.0 ± 1.0	Zrn
258[b]	Leucosome	Contains Sil; boudinaged by D_2; concordant with S_2	50.5 ± 1.0	Zrn, Mnz
Lower level				
292B	Pegmatite	F_2 folded; contains S_2	55.4 ± 3.0	Zrn
60A	Pegmatite	F_2 folded; contains S_2; nearly concordant with S_2	51.8 ± 1.0	Zrn
57	Pegmatite	Igneous fabrics only; highly discordant to S_2	49.5 ± 0.5	Zrn

[a] Mineral abbreviations after Kretz (1983).
[b] U–Pb data presented in Crowley and Parrish (1999).

the sampled layers), whereas others are slightly discordant (Fig. 10). The layers are boudinaged (Fig. 10), typically in orthogonal directions, one of which coincides with the regional stretching direction. They contain a poorly developed layer-parallel S_2 defined by flattened quartz and feldspar. Similar layers that are near the sampled layers (within 100 m) are deformed around fold hinges that are, based on style and orientation, correlated with F_3 structures. These structural relationships suggest that D_2, at least in part, and D_3 occurred after pegmatite and aplite crystallization. Zircons with igneous morphologies were dated from two layers that lie ~5 m apart (Fig. 10). Three zircon analyses from each layer (three to nine grains each; Table 1) yield U–Pb dates that lie slightly below concordia between 52 and 50 Ma (Fig. 8b). Dates from a given layer are similar, differing from dates in the other layer by ~0.5 My.

3.4. Lower level

Sample 57 is from a 0.7 m thick pegmatite dyke that intruded into basement orthogneiss, south of Pettipiece Pass (Fig. 3). The dyke lacks deformation fabrics and is straight and highly discordant to a gneissosity in the host. These relationships suggest that D_2 in the host occurred before pegmatite crystallization. Seven zircon analyses (one to nine grains each; Table 1) lie slightly below concordia between 52 and 49 Ma (Fig. 8b). The youngest analyses lie closest to concordia and the oldest analyses lie farthest away, in a poorly defined array.

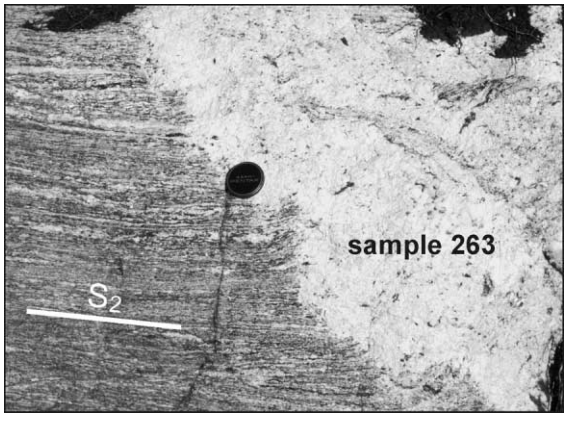

Fig. 9. Sample 263 (56.0 ± 0.5 Ma) is from a pegmatite stock that intruded into amphibolitic gneiss in the upper structural level. The intrusive contacts are highly discordant to S_2 in the host, and the stock lacks ductile deformation fabrics. These relationships suggest that D_2 in the host occurred before intrusion at ~56 Ma. At a lower structural level, D_2 occurred, at least in part, after ~51 Ma (see Fig. 6).

Sample 60A is from a 0.5 m thick pegmatite layer that intruded into basement orthogneiss and granite that is correlated with the 1.85 Ga Bourne granite (Armstrong et al., 1991; Crowley, 1999), south of Pettipiece Pass (Fig. 3). The pegmatite is deformed by folds that partly to completely transposed a Paleoproterozoic gneissosity (age based on cross-cutting relationships of nearby dated Bourne granite (Crowley, 1999)) in the host gneisses into a younger gneissosity (Fig. 11d). The folds are correlated with F_2 folds because they have axial surfaces and hinge lines that parallel such F_2 structures in the adjacent cover sequence rocks. At the collection site on the limb of an isoclinal F_2 fold, flattened quartz and feldspar in the pegmatite layer define a foliation that is parallel and continuous with a gneissosity in the host and slightly discordant to the layer (Fig. 11a–c). These planar fabrics are correlated with S_2 because they parallel S_2 in the adjacent cover sequence rocks. Likewise, a stretching lineation in the layer is correlated with L_2. These relationships suggest that D_2 occurred, at least in part, after pegmatite crystallization. Where the pegmatite truncates 1.85 Ga Bourne granite, the granite layer has a greater discordance with S_2 than the pegmatite layer (Fig. 11a and b). Moreover, the fact that the fabrics in both rocks are correlated with the same D_2 fabrics suggests that they have an identical deformation history. These interpretations require that little, if any, ductile strain occurred between 1.85 Ga and pegmatite crystallization. Six analyses (three to six grains each; Table 1) of zircons with igneous morphologies define two discordias that intersect at the analysis lying closest to concordia (F, Fig. 8c).

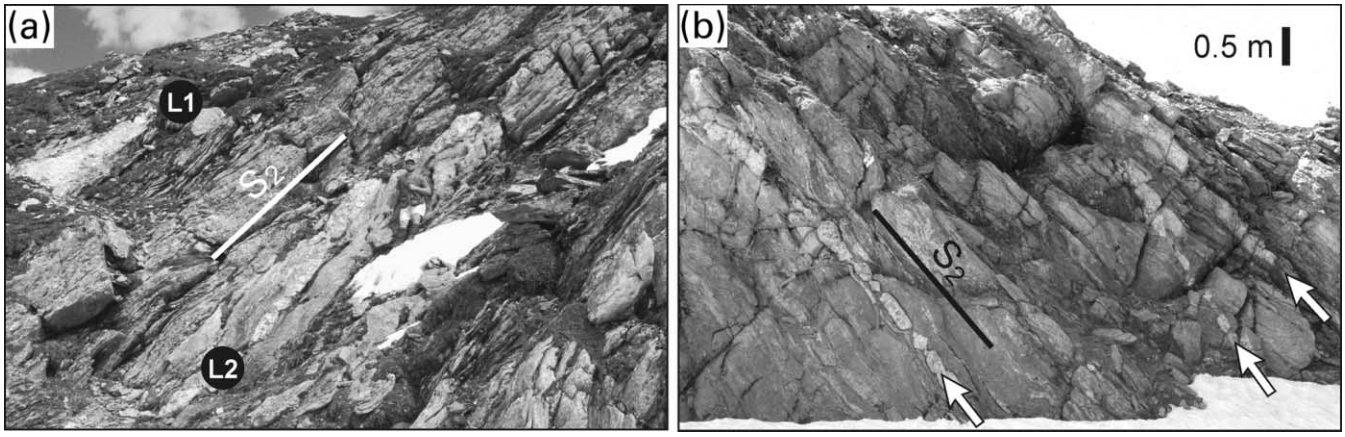

Fig. 10. (a) Sample 12 (51.0 ± 1.0 Ma) is from pegmatite and aplite layers that are boudinaged and concordant with S_2 in the host calcareous schist, in the middle structural level. Two pegmatite layers were collected for dating, the locations of which are denoted by L1 and L2 labels. View is to the east-northeast. (b) The layers in (a) are projected about 10 m to the west into this exposure, which is viewed to the west-southwest. Three pegmatite and aplite layers are denoted by arrows: (from left to right) a boudinaged layer that is concordant with S_2 in the host calcareous schist, a boudinaged layer that is slightly discordant, and a continuous layer that is concordant. These relationships suggest that D_2 occurred, at least in part, after intrusion at ~51 Ma.

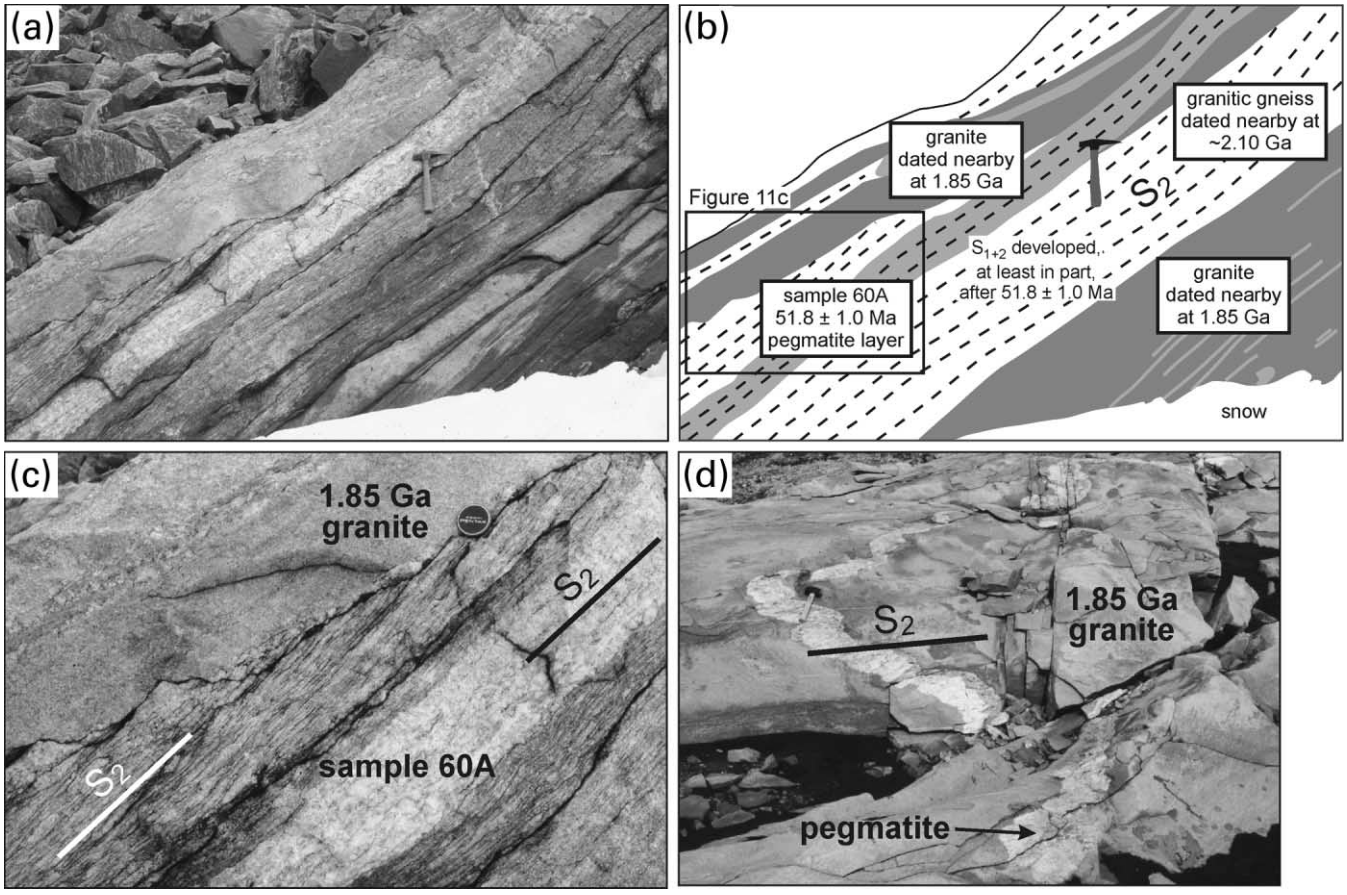

Fig. 11. (a) Sample 60A (51.8 ± 1.0 Ma) is from a pegmatite layer that intruded into granitic orthogneiss and 1.85 Ga Bourne granite in the basement (lower structural level). The pegmatite is nearly concordant with S_2 in the host orthogneiss and contains S_2. These relationships suggest that D_2 occurred, at least in part, after intrusion at ~52 Ma. The interpretation that the Bourne granite appears to have been subjected to the same amount of strain as the pegmatite suggests that there was little, if any, ductile strain between 1.85 Ga and ~52 Ma. View is to the northeast. (b) Line drawing of (a). (c) Detailed view of part of (a), showing details of the fabric relationships. (d) In a locality a few hundred metres from (a), a pegmatite layer that intruded into 1.85 Ga Bourne granite was deformed by F_2 folds. This pegmatite is thought to be coeval with ~52 Ma sample 60A. View is to the northeast, down the plunge of the folds.

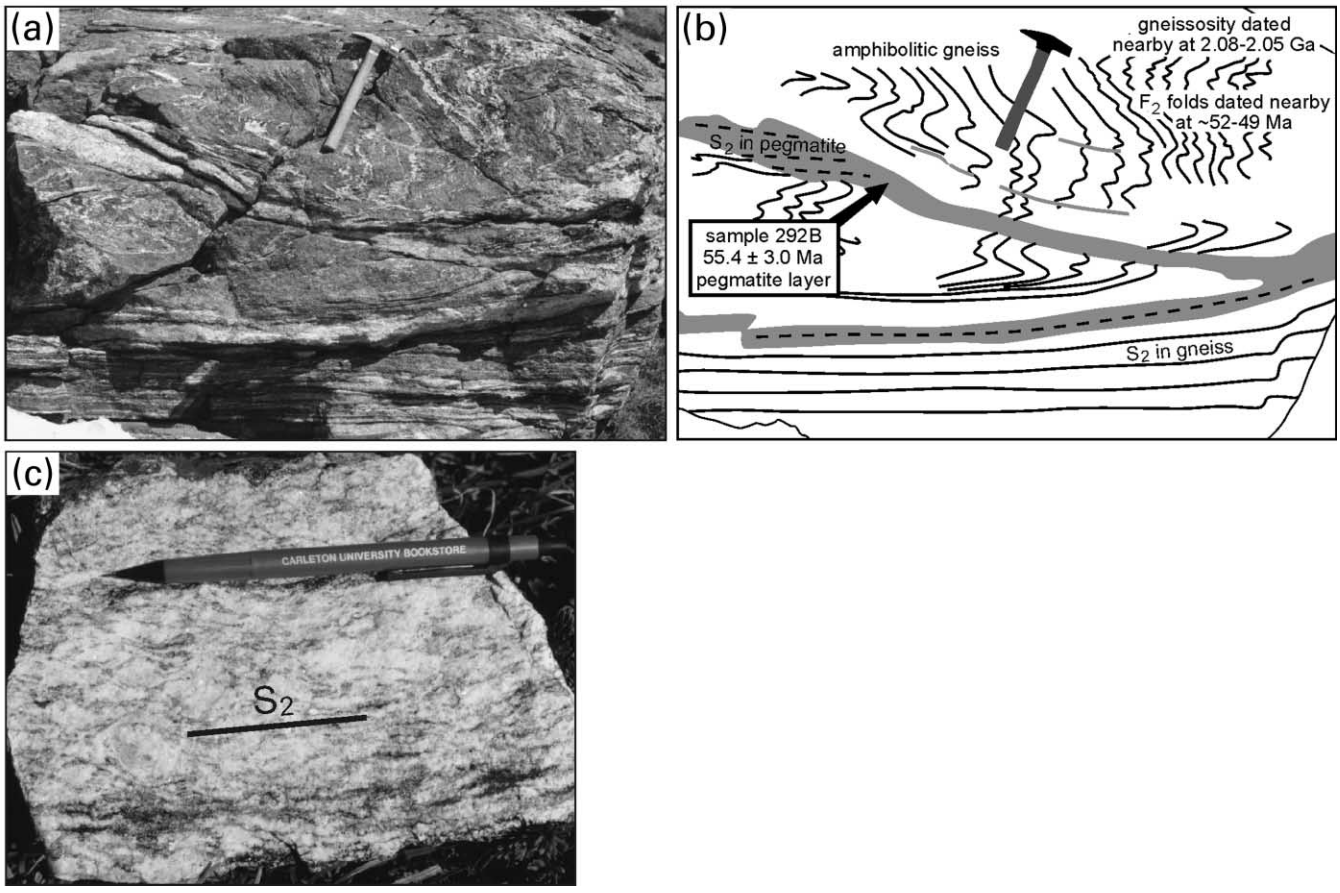

Fig. 12. (a) Sample 292B (55.4 ± 3.0 Ma) is from a pegmatite layer that intruded into basement amphibolitic gneiss in the lower structural level. The layer is discordant to a Proterozoic gneissosity in the host and contains S_2 that is axial planar to F_2 folds (viewed down plunge) that deformed the gneissosity. These relationships suggest that D_2 occurred, at least in part, after intrusion at ~55 Ma. The weakly folded nature of the Proterozoic gneissosity in the upper part of the outcrop suggests that D_2 locally had minor effects. View is to the northeast. (b) Line drawing of (a). (c) Detailed view of S_2 in a handspecimen of pegmatite.

One discordia through three analyses (B, D, F) has upper and lower intercepts of 1767 ± 16 and 51.6 ± 0.2 Ma, respectively (mean square of weighted deviates (MSWD) = 0.1), and the other (A, C, F) has upper and lower intercepts of 2158 ± 116 and 52.0 ± 0.3 Ma, respectively (MSWD = 2.5). The analyses are 98–99% discordant from the upper intercepts.

Sample 292B is from a 0.3 m thick pegmatite layer that intruded into basement amphibolitic gneiss, south of Pettipiece Pass (Fig. 3). The layer is highly discordant to a Paleoproterozoic gneissosity (age based on cross-cutting relationships of nearby 1.85 Ga Bourne granite (Crowley, 1999)) in the host (Fig. 12a and b). The high degree of discordance suggests that the the gneissosity developed before pegmatite crystallization. The pegmatite and gneissosity were deformed by folds that partly to completely transposed the gneissosity into a new orientation (Fig. 12a and b). Flattened quartz and feldspar in the layer define a foliation (Fig. 12c) that is axial planar to the folds, parallel to a younger gneissosity. The folds are correlated with F_2 folds because they have axial surfaces and hinge lines that parallel such F_2 structures in the adjacent cover sequence rocks. Likewise, the younger gneissosity and the foliation in the layer are correlated with S_2. These relationships suggest that D_2 occurred, at least in part, after pegmatite crystallization. Based on the weakly folded nature of the Paleoproterozoic gneissosity in part of the outcrop, the amount of D_2 strain that occurred before crystallization is inferred to be locally minor. Five analyses (one to five grains each; Table 1) of zircons with igneous morphologies define two discordias that contain the analysis lying closest to concordia, which is composed of a single tip of a grain (C, Fig. 8d). One discordia through three analyses (C, B, E) has upper and lower intercepts of 1782 ± 13 and 54.3 ± 2.0 Ma, respectively (MSWD = 85), and another discordia through three analyses (A, C, D) has upper and lower intercepts of 1826 ± 13 and 56.2 ± 2.3 Ma, respectively (MSWD = 115). The analyses are 53–97% discordant from the upper intercepts.

3.5. Age interpretations

The zircon U–Pb analyses plot on concordia diagrams in one of two ways (Fig. 8). Those from samples 12, 57, and

263 plot in clusters that lie slightly below concordia or just overlap it, and those from samples 60A and 292B plot well below concordia in discordant linear arrays with Paleoproterozoic upper intercepts. For the first case, the slight discordance could be caused by combinations of the following: (i) inheritance of a minor amount of xenocrystic zircon; (ii) a small amount of recent Pb loss; (iii) an inherent slight deficiency of ^{206}Pb caused by ^{230}Th fractionation during crystallization (Schärer, 1984; Parrish, 1990), which would decrease the $^{206}Pb/^{238}U$ date by a maximum of 0.1 Ma; or (iv) an inherent slight excess of ^{231}Pa (Schärer, 1984), which would increase the $^{207}Pb/^{235}U$ date.

The position of two analyses from sample 263 pegmatite stock that just overlap concordia at 56 Ma suggests crystallization at that time, and thus we assign an age of 56.0 ± 0.5 Ma. The analyses that plot just above and below 56 Ma are interpreted as containing inheritance and having suffered recent Pb loss, respectively. The analyses from sample 12 pegmatite and aplite layers that lie in two distinct clusters (one cluster each from layers 1 and 2) slightly below concordia between 52 and 50 Ma are difficult to interpret. Although it is possible that the zircons grew at their $^{207}Pb/^{206}Pb$ dates of ~70 Ma and underwent minor recent Pb loss, the tight cluster makes that scenario unlikely because it requires that all grains suffered the identical amounts of Pb loss. Similar reasoning makes it unlikely that all grains contain a minor amount of inherited zircon. We interpret the pegmatite and aplite to have crystallized at a time that corresponds with the part of concordia that lies adjacent to the analyses, and thus we assign an age of 51.0 ± 1.0 Ma. Layer 1 could be slightly younger than layer 2. Slightly discordant analyses from sample 57 pegmatite dyke apparently define a discordia with a lower intercept of ~49.5 Ma. Assuming the discordance is caused by variable amounts of inherited zircon (of a poorly defined Paleoproterozoic age), we assign a crystallization age of 49.5 ± 0.5 Ma.

The significant discordance in samples 60A and 292B pegmatite layers is interpreted as resulting from inheritance of variable amounts of Paleoproterozoic zircon. Igneous crystallization ages are estimated from the lower intercepts of the discordias and inheritance ages are estimated from the upper intercepts. The 51.6 ± 0.2 and 52.0 ± 0.3 Ma lower intercepts of two discordias in sample 60A are used to assign a crystallization age of 51.8 ± 1.0 Ma. Likewise, the 54.3 ± 2.0 and 56.2 ± 2.3 Ma lower intercepts of two discordias in sample 292B are used to assign a crystallization age of 55.4 ± 3.0 Ma. We are confident that the lower intercepts in sample 60A accurately reflect crystallization because the excellent fit to the discordias requires that only two age components are mixed in each analysis, an inherited component of a single age and an igneous component of a single age. The fact that a single analysis (F) is included in both discordias is not contradictory because the lower intercepts agree within error. The analysis that lies between the discordias is thought to contain an intermediate age of inheritance. Less confidence is placed in the lower intercept defined by analyses from sample 292B because the poor fit to the discordias suggests that more than two age components exist in each analysis.

4. Timing of deformation

We interpret the strained states of the dated granitoid rocks as showing that the age of deformation varies with structural level in the Frenchman Cap dome (Figs. 4 and 5; Table 2). In the upper level, the lineated and concordant nature of a leucosome layer (sample 191, Crowley and Parrish (1999)) requires that the synmetamorphic Cordilleran (D_2) deformation occurred, at least in part, after intrusion at ~58 Ma. There are no constraints on the style or amount of deformation that occurred before then (e.g. whether F_1 isoclines developed by then). D_2 is thought to have ceased in some parts of the upper level slightly after ~58 Ma because postdeformational intrusion occurred at ~58 Ma (leucosome, sample 223, Crowley and Parrish (1999)), 56.0 ± 0.5 (pegmatite, sample 263), and ~58–55 Ma (pegmatites, Scammell (1993); Parrish (1995)). These brackets on D_2 are similar to those on the deformation associated with the Monashee décollement on the southern flank of the Thor–Odin dome, where it occurred shortly before ~58 Ma (Carr, 1992).

In structurally lower parts of the middle level, D_2 occurred, at least in part, after intrusion of concordant and boudinaged leucosome (sample 258, Crowley and Parrish (1999)) and pegmatite (sample 12) layers at ~51 and 51.0 ± 1.0 Ma, respectively. D_3 occurred entirely after intrusion of the ~51 Ma pegmatite (sample 12). In the lower level, D_2 occurred, at least in part, after intrusion of foliated and folded pegmatite layers at 55.4 ± 3.0 (sample 292B) and 51.8 ± 1.0 Ma (sample 60A). Although there are no constraints on the style or amount of Cordilleran deformation that occurred before ~52 Ma in the lower level, the fact that sample 60A pegmatite and a layer of 1.85 Ga Bourne granite appear to have the same deformation history suggests that little, if any, Cordilleran ductile strain occurred before pegmatite intrusion at ~52 Ma. D_2 in the lower level must have ceased before intrusion of an undeformed pegmatite (sample 57) at 49.5 ± 0.5 Ma.

The 52–49 Ma ductile deformation in the deeper rocks of the Frenchman Cap dome is correlated with the regional compressional D_2 and D_3 events in higher parts of the dome based on similarities in the orientation and style of folds and associated fabrics. Therefore, compressional D_2 and D_3 in deeper rocks are coeval with the ~53–50 Ma extensional motion on the Columbia River fault (Parkinson, 1992) and the post- ~ 51 Ma extensional motion on the Okanagan–Eagle River fault system (Parrish et al., 1988). This temporal overlap requires that extensional deformation above the dome was synchronous with compressional deformation in deeper parts.

5. Strain gradient

We interpret the strained states of the dated granitoid rocks as showing that a Cordilleran strain gradient exists between highly strained cover sequence rocks and weakly strained basement rocks in the Frenchman Cap dome (Figs. 4 and 5; Table 2). The highly strained state of Proterozoic rocks that lie in the upper structural level (samples 180, 187, 207, Crowley (1997)) (Fig. 6a) and middle level (sample 341, Crowley (1997)) indicates that D_2 substantially affected these parts of the dome. In contrast, relationships between ~52 Ma pegmatite layers (samples 60A and 292B), 1.85 Ga Bourne granite layers, and a pre-1.85 Ga gneissosity (Figs. 11 and 12) indicate that deformation between 1.85 Ga and ~52 Ma was relatively insignificant in higher parts of the lower level. The presence of weakly deformed and undeformed Paleoproterozoic dykes (samples 84, 91, 308, Crowley (1999)) indicates that D_2 was locally weak to nonexistent in deep exposures in the lower level. The D_2 gradient is tightest near the contact between the uppermost basement paragneiss horizon, which contains a gneissosity (Fig. 6b) and a lineation that are correlated with S_2 and L_2, respectively, and the underlying basement orthogneisses, which preserve a Paleoproterozoic gneissosity and discordant intrusive contacts.

Cordilleran D_2 strain in the basement was partitioned at various scales into high and low strain domains according to rock type, and thus did not follow a simple gradient. The timing of deformation in the basement is obviously best known in the limited areas with U–Pb data, but for the purpose of making the conclusions that are presented next, it was necessary to extrapolate from these areas. Extrapolation was largely made by using layers of 1.85 Ga Bourne granite, which are the most important structural markers in the dome becaused of their distinctive appearance and ubiquitous nature and the fact that they were undeformed before Cordilleran orogenesis.

Basement paragneiss is interpreted as having been strongly affected by D_2 because it contains a single foliation (Fig. 6b) that is correlated, based on similar orientation, with S_2. In addition to being affected by D_2, the paragneiss was locally affected by F_3 folds that are rare in surrounding orthogneiss but well developed in the cover sequence on the east side of the dome. In contrast to the paragneiss, orthogneiss varies on a decimetre to metre scale from containing only a steeply dipping Proterozoic gneissosity, to containing a Proterozoic gneissosity and a shallowly dipping S_2 gneissosity, to containing only a S_2 gneissosity. An example of these fabric variations is shown in Fig. 13. The S_2 gneissosity is correlated with S_2 in the cover sequence on the basis of similar orientation and the fact that it is axial planar to folds that are correlated with F_2 folds on the basis of style and orientation. S_2 formed during the reorientation and shearing of the Proterozoic gneissosity during F_2 folding and from fabric development and leucosome generation in the axial surfaces of F_2 folds (Fig. 13). It is best developed on the limbs of tight to isoclinal F_2 folds and where the Proterozoic gneissosity had a preexisting orientation that is axial planar to F_2 folds. D_2 appears to have had the least effect in amphibolitic gneiss (e.g. host to sample 292B pegmatite (Fig. 12)), where the Proterozoic gneissosity is typically only significantly reoriented in the limbs of rare tight F_2 folds.

6. Tectonic model

Key observations that are central to any tectonic model for the dome include: the inverted metamorphic sequence in the higher rocks of the Frenchman Cap dome (Journeay, 1986 and references therein), the downward younging of deformation (this study) and metamorphism (Crowley and Parrish, 1999) through the dome, and the strain gradient (this study).

Inverted metamorphic sequences have been documented in many orogenic belts (e.g. LeFort, 1975; Spear et al., 1995); their existence poses the question as to whether the associated thermal gradient was inverted rather than normal. Proving that an inverted sequence was accompanied by an inverted thermal gradient is a relatively easy task in rocks that were only weakly deformed after the onset of metamorphism (e.g. rocks in the contact aureole of a shallow undeformed pluton). In rocks that were deformed during or after metamorphism, however (e.g. rocks in the Frenchman Cap dome) it is difficult to demonstrate that an inverted gradient existed because it cannot be assumed that the rocks attained their thermal peak in approximately their present relative positions. Modeling has shown how an inverted metamorphic sequence can form in the absence of an inverted thermal gradient if there were substantial syn- to post-metamorphic displacements within it. For example, Jamieson et al. (1996) showed that an inverted sequence could form by tectonic juxtaposition of rocks that had widely varying initial positions and reached peak temperatures at different places and times within the orogen. The juxtaposition is capable of telescoping a previously laterally extensive normal sequence into a stacked inverted sequence without ever placing warmer rocks over cooler rocks.

Crowley and Parrish (1999) concluded that structurally higher rocks in the Frenchman Cap dome cannot have been the heat source for metamorphism in deeper rocks because their U–Pb dating and $^{40}Ar/^{39}Ar$ dating of Sanborn (1996) showed that higher rocks attained peak temperatures and cooled rapidly while deeper rocks heated toward a thermal peak that was attained a few million years later. Gibson et al. (1999) came to the same conclusion based on U–Pb data (Gibson, 1997) and structural data from the northernmost part of the dome. We follow the model of Gibson et al. (1999) by proposing that the inverted sequence in the upper part of the dome and the downward younging in thermal peak ages through the dome resulted from the synmetamorphic juxtaposition of rocks that were heated at

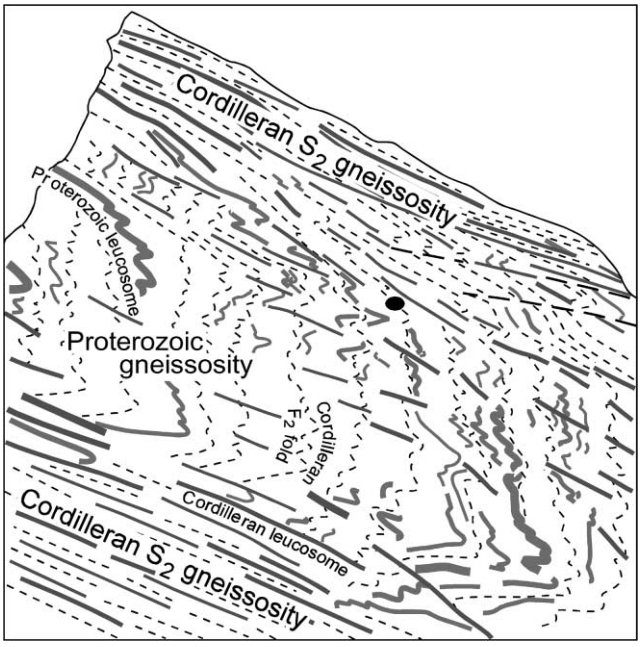

Fig. 13. Sketch from a photograph showing fabric relationships in the basement orthogneiss. The scale is a camera lens cap near the centre of the sketch (50 mm). A migmatitic gneissosity is deformed by folds (viewed down plunge) with an axial planar foliation. The folded gneissosity is interpreted as Proterozoic based on nearby U–Pb dating, the folds are interpreted as Cordilleran F_2 folds based on nearby U–Pb dating and similarity in style and orientation, and the axial planar foliation is interpreted as the Cordilleran S_2. S_2 is a composite transposition foliation that resulted from reorientation of the Proterozoic gneissosity via F_2 folding and leucosome generation in the axial surfaces of the folds. These relationships indicate that D_2 strain in the basement varies greatly on a decimetre to metre scale.

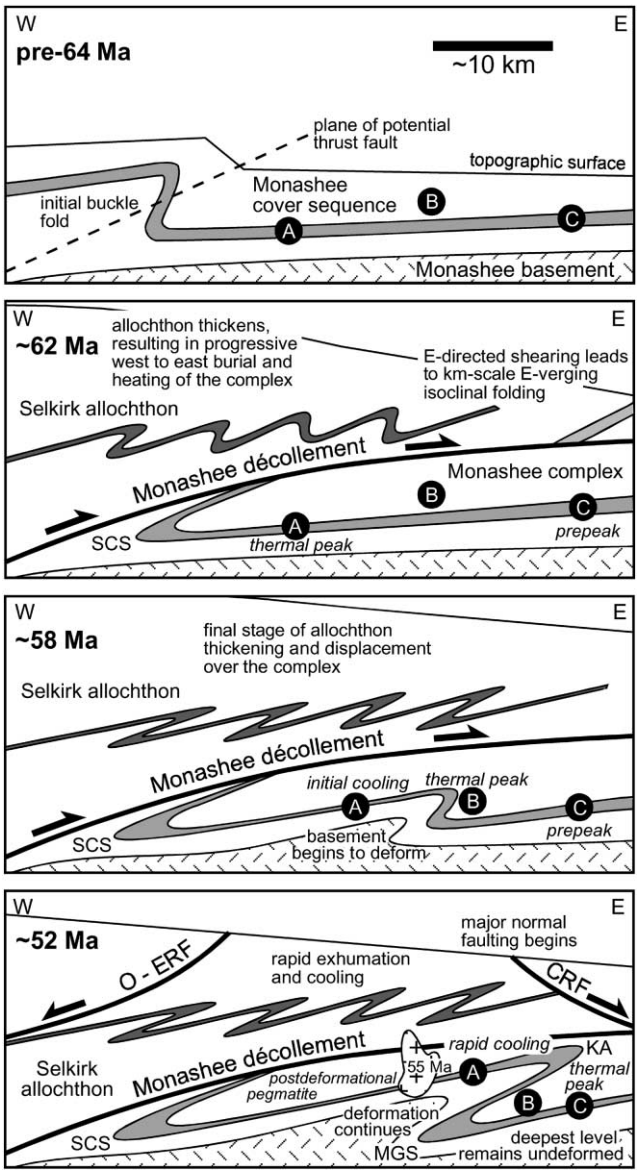

Fig. 14. Tectonic model for the Frenchman Cap dome, modified after Gibson et al. (1999). Schematic cross-sections that represent the inferred crustal structure and metamorphic conditions at four times show how rocks (denoted by locations A–C) that were initially greatly separated from east to west before 64 Ma were structurally telescoped by ~52 Ma, largely during development of kilometre-scale east-verging F_1 isoclines (Sibley Creek syncline (SCS), Kirbyville anticline (KA), Mount Grace syncline (MGS)). Stretching of the isocline limbs has been included in the model, but faulting along the limbs, such as along the Ratchford Creek and Anstey Range faults, has not been considered because the displacements are unknown. Major Eocene normal faults are shown (Columbia River fault (CRF), Okanagan–Eagle River fault (O–ERF)).

different places and times within the orogen. In this model, schematically depicted in Fig. 14, a normal metamorphic sequence that initially extended a significant distance (at least a few tens of kilometres) to the west of the presently exposed basement in the centre of the dome was telescoped into the present 6 km thick sequence. The telescoping is thought to have been mainly accomplished by east-verging kilometre-scale F_1 isoclinal folding and shearing along surfaces that parallel the isocline limbs, such as the Ratchford Creek and Anstey Range faults. In order for the thermal gradient to have remained normal, final emplacement of the higher rocks must have occurred after they cooled below the temperatures of the deeper rocks. We build upon the model of Gibson et al. (1999) by proposing that the pattern of downward younging deformation ages is also attributed to tectonic juxtaposition; rocks to the west that were already substantially deformed were emplaced onto those that underwent less total strain at a younger time (Fig. 14).

An important part of this model is that F_1 isoclines developed during the thermal peak of metamorphism; F_1 isoclines are interpreted as being responsible for much of the tectonic juxtaposition, and thus cannot be prepeak structures if our model is correct. The isoclines were previously mapped as prepeak structures based on the interpretation that they were overprinted by the synpeak outcrop-scale F_2 folds. There are no data or observations, however, that preclude the possibility that the isoclines formed near or at the thermal peak and were developing during F_2 folding. A substantial amount of east-directed translation of structurally higher parts of the cover sequence over the

deeper parts is another important part of this model; substantial translation allows higher rocks to have been metamorphosed and deformed a significant distance to the west of the deeper rocks before juxtaposition. Stratigraphic marker horizons in the cover sequence are apparently continuous through the dome (Figs. 3 and 4), which could suggest that higher rocks were displaced less than a few kilometres relative to the deeper rocks. Given that the horizons are sheared and extensively thinned along the limbs of the isoclines, however, the apparent continuity does not constrain the amount of east-directed displacement, other than requiring that it was probably less than many tens of kilometres.

Brown et al. (1986) and Journeay (1986) inferred that Cordilleran thrust faults or ductile shear zones exist beneath rocks exposed in the Frenchman Cap dome. The presence of a D_2 strain gradient documented here suggests, however, that the base of significant Cordilleran deformation may instead lie in basement rocks exposed in the dome. Investigation of deeper structural levels than those exposed in the study area may resolve this issue. Our reconnaissance mapping in the southern part of the dome, in perhaps the structurally deepest rocks in the dome, indicates that Cordilleran deformation was rather weak (i.e. fabrics of inferred Paleoproterozoic age are not completely transposed). The conclusion that the base of significant Cordilleran deformation lies in exposed basement rocks supports the notion that the Monashee complex is autochthonous, and thus has always been part of the North American craton, as was proposed based on the ages of the basement rocks (Crowley, 1999 and references therein).

Attainment of peak temperatures in deeper rocks occurred during motion on overlying major Eocene normal fault systems, such as the Columbia River and Okanagan–Eagle River faults. This temporal overlap may explain why deeper rocks were: (i) at peak temperatures for a short duration, perhaps only a few million years (Crowley and Parrish, 1999), and (ii) locally unaffected by D_2. In other words, it is possible that the D_2 strain gradient was preserved because the basement attained elevated temperatures and began deforming when the tectonic regime changed from compressional to extensional. Once in an extensional regime, the basement rocks underwent rapid exhumation and subsequent cooling, and thus they did not experience the long duration needed to transpose Paleoproterozoic structures into a Cordilleran orientation. If this had not been the case, the basement rocks would have continued to have been buried, heated, and compressed, resulting in rocks that would have been as strongly strained as those at higher levels and a strain gradient that would lie below presently exposed basement.

A Cordilleran strain gradient in the basement is a key part of a recently proposed tectonic model for the Thor–Odin dome (Johnston et al., 2000), but thus far no evidence has been found and Vanderhaeghe et al. (1999) proposed that deep levels of the dome were heavily infiltrated with anatectic melts at ~56 Ma. We suggest that presently exposed basement rocks in the Thor–Odin dome were heated for a longer time or at an earlier time than those in the Frenchman Cap dome, resulting in a higher degree of strain and a deeper, presently unexposed, strain gradient in Thor–Odin. In support of this suggestion, we note that the sparse U–Pb data from Thor–Odin basement (Vanderhaeghe et al., 1999; Johnston et al., 2000) indicates that peak temperatures were attained 5–6 My before those in the Frenchman Cap basement, a few million years before the onset of extension.

Compositional differences between cover and basement rocks may have played a role in formation of the strain gradient; basement is mainly composed of orthogneiss that was tectonized in the Paleoproterozoic, and therefore may have been more resistant to Cordilleran strain than cover rocks that were low grade supracrustal rocks before the Tertiary. Likewise, compositional differences between Frenchman Cap and Thor–Odin basement rocks may have contributed to differences in the amount of strain recorded in each dome; Frenchman Cap basement is largely composed of orthogneiss with little paragneiss, whereas Thor–Odin dome is dominated by paragneiss.

7. Conclusions

Structural relationships of dated granitoid rocks in a 6-km-thick section of Frenchman Cap dome were used to place constraints on the age and intensity of deformation beneath the Selkirk allochthon, in one of the deepest structural exposures in the southern Canadian Cordillera. At high structural levels, immediately beneath the Monashee décollement that transported the allochthon eastward, a metasedimentary-dominated cover sequence was strongly affected by kilometre-scale east-verging isoclinal folds (F_1) and outcrop-scale tight-to-isoclinal folds (F_2) that are associated with the dominant foliation and lineation. This F_2 folding, at least in part, occurred at 58–55 Ma. In deeper levels of the cover sequence and the underlying orthogneiss-dominated basement, F_2 folding, at least in part, occurred at 52–49 Ma. Paleoproterozoic dykes in the basement were locally weakly affected by D_2. These new findings require that: (i) D_2 compression youngs structurally downward, synchronous with the thermal peak of metamorphism (Crowley and Parrish, 1999); (ii) D_2 in deeper levels is synchronous with extension above the complex that was partly responsible for its exhumation (Parrish et al., 1988 and references therein); and (iii) a D_2 strain gradient lies between strongly deformed cover rocks and weakly D_2 deformed basement.

We incorporate these interpretations into a model (Fig. 14) in which rocks that were tectonised at different places and times within the orogen were juxtaposed, likely during east-verging kilometre-scale F_1 folding and shearing along the isocline limbs. A similar model was proposed by Gibson

et al. (1999) to explain a pattern of downward younging thermal peak ages and an inverted metamorphic sequence in higher rocks. The rapid downward decrease in deformation intensity suggests that the lower limit of significant Cordilleran deformation lies in basement rocks exposed in the Frenchman Cap dome, and thus the Monashee complex has always been part of the North American craton (Crowley, 1999 and references therein). Cessation of deformation at this structural level is attributed to the fact that the basement attained elevated temperatures and began straining when the Cordilleran tectonic regime changed from compressional to extensional. A Cordilleran strain gradient has not yet been recognized in the Thor–Odin dome, suggesting that one may exist at a deeper, unexposed structural level. Differences between the Thor–Odin and the Frenchman Cap domes might be attributed to the fact that basement rocks in the former appear to have been heated for a longer time or at an earlier time than those in the latter.

Acknowledgements

This work is part of a PhD thesis undertaken by JLC at Carleton University and supervised by RLB and RRP. Fieldwork was supported by the Geological Survey of Canada (GSC) and by Natural Sciences and Engineering Research Council of Canada (NSERC) research grants to RLB and RRP. U–Pb geochronology at Carleton University was supported by NSERC research grants primarily to S.D. Carr, and also to RLB and RRP. We are grateful to S.D. Carr for providing advice and materials needed for the U–Pb dating. Mass spectrometry was supported by the GSC. P.M. Schaubs, D.H. Gibson and N.M. Sanborn are thanked for field assistance. Insightful comments by D.J. Scott and an anonymous reviewer were helpful.

References

Armstrong, R.L., Parrish, R.R., van der Heyden, P., Scott, K., Runkle, D., Brown, R.L., 1991. Early Proterozoic basement exposures in the southern Canadian Cordillera: core gneiss of Frenchman Cap. Unit I of the Grand Forks Gneiss and Vaseaux Formation. Canadian Journal of Earth Sciences 28, 1169–1201.

Brown, R.L., 1980. Frenchman Cap dome, Shuswap complex, British Columbia: a progress report. In: Current Research, part A, Geological Survey of Canada Paper 80-1A, pp. 47–51.

Brown, R.L., Journeay, J.M., 1987. Tectonic denudation of the Shuswap metamorphic terrane of southeastern British Columbia. Geology 15, 142–146.

Brown, R.L., Journeay, J.M., Lane, L.S., Murphy, D.C., Rees, C.J., 1986. Obduction, backfolding and piggyback thrusting in the metamorphic hinterland of the southeastern Canadian Cordillera. Journal of Structural Geology 8, 225–268.

Brown, R.L., Carr, S.D., Johnson, B.J., Coleman, V.J., Cook, F.A., Varsek, J.L., 1992. The Monashee décollement of the southern Canadian Cordillera: a crustal-scale shear zone linking the Rocky Mountain Foreland belt to lower crust beneath accreted terranes. In: McClay, K.R. (Ed.). Thrust Tectonics. Chapman and Hall, London, UK, pp. 357–364.

Brown, R.L., Beaumont, C., Willett, S.D., 1993. Comparison of the Selkirk fan structure with mechanical models: implications for interpretation of the southern Canadian Cordillera. Geology 21, 1015–1018.

Carr, S.D., 1992. Tectonic setting and U–Pb geochronology of the early Tertiary Ladybird leucogranite suite, Thor–Odin–Pinnacles area, southern Omineca Belt, British Columbia. Tectonics 11, 258–278.

Carr, S.D., 1995. The southern Omineca Belt, British Columbia: new perspectives from the Lithoprobe Geoscience Program. Canadian Journal of Earth Sciences 32, 1720–1739.

Coleman, V.J., 1990. The Monashee décollement at Cariboo Alp and regional kinematic indicators, southeastern British Columbia. MSc thesis, Carleton University.

Cook, F.A., Varsek, J.L., Clowes, R.M., Kanasewich, E.R., Spencer, C.S., Parrish, R.R., Brown, R.L., Carr, S.D., Johnson, B.J., Price, R.A., 1992. Lithoprobe crustal reflection cross-section of the southern Canadian Cordillera, 1, Foreland thrust and fold belt to Fraser River fault. Tectonics 11, 12–35.

Crowley, J.L., 1997. U–Pb geochronologic constraints on the cover sequence of the Monashee complex, Canadian Cordillera: Paleoproterozoic deposition on basement. Canadian Journal of Earth Sciences 34, 1008–1022.

Crowley, J.L., 1999. U–Pb geochronologic constraints on Paleoproterozoic tectonism in the Monashee complex, Canadian Cordillera: elucidating an overprinted geologic history. Geological Society of America Bulletin 111, 560–577.

Crowley, J.L., Parrish, R.R., 1999. U–Pb isotopic constraints on diachronous metamorphism in the northern Monashee complex, southern Canadian Cordillera. Journal of Metamorphic Geology 17, 483–502.

Gibson, H.D., 1997. Thermotectonic evolution of the northern Monashee complex, southern Omineca Belt, southeastern British Columbia. MSc thesis, Carleton University.

Gibson, H.D., Brown, R.L., Parrish, R.R., 1999. Deformation-induced metamorphic field gradients: an example from the southeastern Canadian Cordillera. Journal of Structural Geology 21, 751–767.

Höy, T., Brown, R.L., 1980. Geology of eastern margin of Shuswap complex, Frenchman Cap area. British Columbia Ministry of Energy, Mines and Petroleum Resources Preliminary Map 43, scale 1:100,000.

Höy, T., Godwin, C.I., 1988. Significance of a Cambrian date from galena lead-isotope data for the stratiform Cottonbelt deposit in the Monashee complex, southeastern British Columbia. Canadian Journal of Earth Sciences 25, 1534–1541.

Jamieson, R.A., Beaumont, C., Hamilton, J., Fullsack, P., 1996. Tectonic assembly of inverted metamorphic sequences. Geology 24, 839–842.

Johnson, B.J., Brown, R.L., 1996. Crustal structure and early Tertiary extensional tectonics of the Omineca belt at 51°N latitude, southern Canadian Cordillera. Canadian Journal of Earth Sciences 33, 1596–1611.

Johnston, D.H., Williams, P.F., Brown, R.L., Crowley, J.L., Carr, S.D., 2000. Northeastward extrusion and extensional exhumation of crystalline rocks of the Monashee complex, southeastern Canadian Cordillera. Journal of Structural Geology 22, 603–625.

Journeay, J.M., 1986. Stratigraphy, internal strain, and thermo-tectonic evolution of northern Frenchman Cap dome, an exhumed basement duplex structure, Omineca hinterland, southeastern Canadian Cordillera. PhD thesis, Queen's University.

Kretz, R., 1983. Symbols for rock forming minerals. American Mineralogist 68, 277–279.

Krogh, T.E., 1982. Improved accuracy of U–Pb ages by the creation of more concordant systems using an air abrasion technique. Geochimica et Cosmochimica Acta 46, 637–649.

Lane, L.S., 1984. Deformation history of the Monashee décollement and Columbia River fault zone, British Columbia. PhD thesis, Carleton University.

LeFort, P., 1975. Himalayas: the collided range: present knowledge of the continental arc. American Journal of Science 275A, 1–44.

McNicoll, V.J., Brown, R.L., 1995. The Monashee décollement at Cariboo

Alp, southern flanks of the Monashee complex, southern British Columbia, Canada. Journal of Structural Geology 17, 17–30.

Monger, J.W.H., Price, R.A., Tempelman-Kluit, D.J., 1982. Tectonic accretion and the origin of the two major metamorphic and plutonic welts in the Canadian Cordillera. Geology 10, 70–75.

Parkinson, D.L., 1992. Age and tectonic evolution of the southern Monashee complex, southeastern British Columbia: a window into the deep crust. PhD thesis, University of Santa Barbara.

Parrish, R.R., 1987. An improved micro-capsule for zircon dissolution in U–Pb geochronology. Chemical Geology 66, 99–102.

Parrish, R.R., 1990. U–Pb dating of monazite and its applications to geological problems. Canadian Journal of Earth Sciences 27, 1431–1450.

Parrish, R.R., 1995. Thermal evolution of the southeastern Canadian Cordillera. Canadian Journal of Earth Sciences 32, 1618–1642.

Parrish, R.R., Krogh, T.E., 1987. Synthesis and purification of ^{205}Pb for U–Pb geochronology. Chemical Geology 66, 103–110.

Parrish, R.R., Roddick, J.C., Loveridge, W.D., Sullivan, R.W., 1987. Uranium–lead analytical techniques at the Geochronology Laboratory. In: Radiogenic age and isotopic studies, Report 1, Geological Survey of Canada Paper 87-2, pp. 3–7.

Parrish, R.R., Carr, S.D., Parkinson, D.L., 1988. Eocene extensional tectonics and geochronology of the southern Omineca Belt, British Columbia and Washington. Tectonics 7, 181–212.

Read, P.B., Brown, R.L., 1981. Columbia River fault zone: southeastern margin of the Shuswap and Monashee complexes, southern British Columbia. Canadian Journal of Earth Sciences 18, 1127–1145.

Roddick, J.C., 1987. Generalized numerical error analysis with applications to geochronology and thermodynamics. Geochimica et Cosmochimica Acta 51, 2129–2135.

Roddick, J.C., Loveridge, W.D., Parrish, R.R., 1987. Precise U/Pb dating of zircon at the sub-nanogram Pb level. Chemical Geology 66, 111–121.

Sanborn, N.M., 1996. Constraints on the timing and conditions of Cordilleran tectonism in Frenchman Cap dome, Monashee complex, southeast British Columbia, from ^{40}Ar/^{39}Ar geochronology. BSc thesis, Queens University.

Scammell, R.J., 1986. Stratigraphy, structure, and metamorphism of the north flank of the Monashee complex, southeastern British Columbia: a record of Proterozoic extension and Phanerozoic crustal thinning. MSc thesis, Carleton University.

Scammell, R.J., 1993. Mid-Cretaceous to Tertiary thermotectonic history of former mid-crustal rocks, southern Omineca Belt, Canadian Cordillera. PhD thesis, Queens University.

Scammell, R.J., Brown, R.L., 1990. Cover gneisses of the Monashee Terrane: a record of synsedimentary rifting in the North American Cordillera. Canadian Journal of Earth Sciences 27, 712–726.

Schärer, U., 1984. The effect of initial 230Th disequilibrium on young U–Pb ages: the Makalu case, Himalaya. Earth and Planetary Science Letters 67, 191–204.

Spear, F.S., Kohn, M.J., Paetzold, S., 1995. Petrology of the regional sillimanite zone, west-central New Hampshire, USA, with implications for the development of inverted isograds. American Mineralogist 80, 361–376.

Steiger, R.H., Jäger, E., 1977. Subcommision on geochronology: convention on the use of decay constants in geo- and cosmochronology. Earth and Planetary Science Letters 36, 359–362.

Vanderhaeghe, O., Teyssier, C., Wysoczanski, R., 1999. Structural and geochronological constraints on the role of partial melting during the formation of the Shuswap metamorphic core complex at the latitude of the Thor–Odin dome, British Columbia. Canadian Journal of Earth Sciences 36, 917–943.

Wheeler, J.O., 1965. Big Bend map area, British Columbia (82N east half). Geological Survey of Canada Paper 64-32, 37pp.

Wheeler, J.O., McFeely, P. (compilers), 1991. Tectonic assemblage map of the Canadian Cordillera and adjacent parts of the United States of America, scale 1:2,000,000. Geological Survey of Canada Map 1712A.

York, D., 1969. Least squares fitting of a straight line with correlated errors. Earth and Planetary Science Letters 5, 320–324.